Figure 1

Alignment of sequences

Sequences of the antibodies of the present invention are given below.
SEQ ID NO. is listed in parentheses to the right of the sequence.
CDR1, CDR2 and CDR3 according to Kabat are highlighted: sequences in italics represent CDR1, underlined sequences represent CDR2, bold sequences represent CDR3.

VH:



QVQLVESGGGVVQPGRSLRLSCAASGFTFSDYAMHWVRQAPGKGLEWVAVIPYDGDNKYYADSVKGRFTISRDNSKNTLYLQMNSLRAEDTAVYYCAREDWG-------LEVDYWGQGALVTVSS VH1015-044(41)

EVQLVQSGAEVKKPGESLKISCKGSGYSFTSYWIGWVRQMPGKGLEWMGIIYPGDSDTRYSPSFQGQVTISADKSISTAYLQWSSLKASDTAMYYCARHKLGMDHD----AFDIWGQGTMVTVSS VH1015-087(45)

QVQLVQSGAEVRKPGSSVKVSCKASGGSFNWYFIFWVRQAPGQGFEWMGRIIPILGITAYAQKFQGRVTITADKSTSTAYMELNSLRSEDTAVYYCAGGDD------LD--AFDIWGQGTMVSVSS VH1015-098(49)

QVQLVESGGGVVQPGRSLRLSCAGSGFTFNRYAMYWVRQAPGKGLDWVAVISNDGINKYYADSVKGRFTISRDNSKNTLYLQMNSLRAEDTAVYYCARDHTMV-----RGAFDYWGQGTLVTVSS VH1015-111(53)

Figure 1 continued...

VL:

```
                                |-CDR1--|                 |CDR2|                                                                                                  |---CDR3----|
DIQMTQSPSSLSASVGDRVTITCRASQGISR-WLAWYQQKPEKAPKSLIYAASSLQSGVPSRFSGSGSGTDFTLTISSLQPEDFATYYCQQYDSDP-ITFGQGTRLEIK VL1015-013 (57)
EIVLTQSPGTLSLSPGERATLSCRASQSVSSSYLAWYQQKPGQAPRLLIYGASRATGIPDRFSGSGSGTDFTLTISRLEPEDFAVYYCQQYGSS--LTFGGGTKVEIK VL1015-114 (61)
DIQMTQSPPSLSASAGDRVTITCRASQGISS-RLAWYQQKPEKAPKSLIYAASSLQSGVPSRFSGSGSGTDFTLTISSLQPEDFATYYCQQYNSYP-YTFGQGTKLEIK VL1015-011 (65)
EIVLTQSPGTLSLSPGERATLSCRASQSVRSSYLAWYQQKPGQAPRLLIYGASRATGIPDRFSGSGSGTDFTLTISRLEPEDFAVYYCQQYGSSP-RTFGQGTKVEIK VL1015-017 (69)
EIVLTQSPGTLSLSPGERATLSCRASQSVGSSSLAWYQQKPGQAPRLLIYGASRATGIPDRFSGSGSGTDFTLTISRLEPEDFAVYYCQQYGSSP-RWTFGQGTKVEIK VL1015-042 (73)
DIQMTQSPSSLSASVGDRVTITCRASQGISS-RLAWYQQKPEKAPKSLIYAASSLQSGVPSRFSGSGSGTDFTLTISSLQPEDFATYYCQQYNSYP-YTFGQGTKLEIK VL1015-092 (77)
DIQMTQSPSSLSASVGDRVTITCRASQGISS-WLAWYQQKPEKAPKSLIYAASSLQSGVPSRFSGSGSGTDFTLTISSLQPEDFATYYCQQYNSYPLYTFGQGTKLEIK VL1015-101 (81)
AIQLTQSPSSLSASVGDRVTITCRASQDISS-ALAWYQQKPGKAPKLLIYDASILESGVPSRFSGSGSGTDFTLTISSLQPEDFATYYCQQFNSYP-LTFGGGTKVEIK VL1015-003 (85)
EIVLTQSPATLSLSPGERATLSCRASQSVSS-YLAWYQQKPGQAPRLLIYDASNRATGIPARFSGSGSGTDFTLTISSLEPEDFAVYYCQQRSNWP-LTFGGGTKVEIK VL1015-025 (89)
EIVLTQSPATLSLSPGERAILSCRASQSVSS-YLAWYQQKPGQAPRLLIYDASNRATGIPARFSGSGSGTDFTLTISSLEPEDFAVYYCQQRSNWP-LTFGGGTKVEIK VL1015-109 (93)
AIQLTQSPSSLSASVGDRVTITCRASQGINS-ALAWYQQKPGKAPKLLIYDASSLESGVPSRFSGSGSGTDFTLTISSLQPEDFATYYCQQFNSYP-LTFGGGTKVEIK VL1015-044 (97)
DIQMTQSPSSLSASVGDRVTITCRASQGISS-WLAWYQQKPEKAPKSLIYAASSLQSGVPSRFSGSGSGTDFTLTISSLQPEDFATYYCQQYNSYP-PTFGQGTVEVK VL1015-087 (101)
DIQMTQSPSSLSASVGDRVTITCRASQGISS-WLAWYQQKPEKAPKSLIYAASSLQSGVPSRFSGSGSGTDFTLTISSLQPEDFATYYCQQYNSYP-YTFGQGTKLEIK VL1015-098 (105)
EIVLTQSPATLSLSPGERATLSCRASQSVSS-YLAWYQQKPGQAPRLLIYDASNRATGIPARFSGSGSGTDFTLTISSLEPEDFAVYYCQQRSNWP-LTFGGGTKVEIK VL1015-111 (109)
```

Figure 2

SEQ ID NO: 113: The amino acid sequence of the wildtype C_H region of human IgG4.

```
  1 ASTKGPSVFP LAPCSRSTSE STAALGCLVK DYFPEPVTVS WNSGALTSGV
 51 HTFPAVLQSS GLYSLSSVVT VPSSSLGTKT YTCNVDHKPS NTKVDKRVES
101 KYGPPCPSCP APEFLGGPSV FLFPPKPKDT LMISRTPEVT CVVVDVSQED
151 PEVQFNWYVD GVEVHNAKTK PREEQFNSTY RVVSVLTVLH QDWLNGKEYK
201 CKVSNKGLPS SIEKTISKAK GQPREPQVYT LPPSQEEMTK NQVSLTCLVK
251 GFYPSDIAVE WESNGQPENN YKTTPPVLDS DGSFFLYSRL TVDKSRWQEG
301 NVFSCSVMHE ALHNHYTQKS LSLSLGK
```

The Sequence in italics represents the CH1 region, highlighted sequence represents the hinge region, regular sequence represents the CH2 region and underlined sequence represents the CH3 region.

SEQ ID NO: 114: The amino acid sequence of the hingeless C_H region of a human IgG4.

```
  1 ASTKGPSVFP LAPCSRSTSE STAALGCLVK DYFPEPVTVS WNSGALTSGV
 51 HTFPAVLQSS GLYSLSSVVT VPSSSLGTKT YTCNVDHKPS NTKVDKRVAP
101 EFLGGPSVFL FPPKPKDTLM ISRTPEVTCV VVDVSQEDPE VQFNWYVDGV
151 EVHNAKTKPR EEQFNSTYRV VSVLTVLHQD WLNGKEYKCK VSNKGLPSSI
201 EKTISKAKGQ PREPQVYTLP PSQEEMTKNQ VSLTCLVKGF YPSDIAVEWE
251 SNGQPENNYK TTPPVLDSDG SFFLYSRLTV DKSRWQEGNV FSCSVMHEAL
301 HNHYTQKSLS LSLGK
```

Figure 3

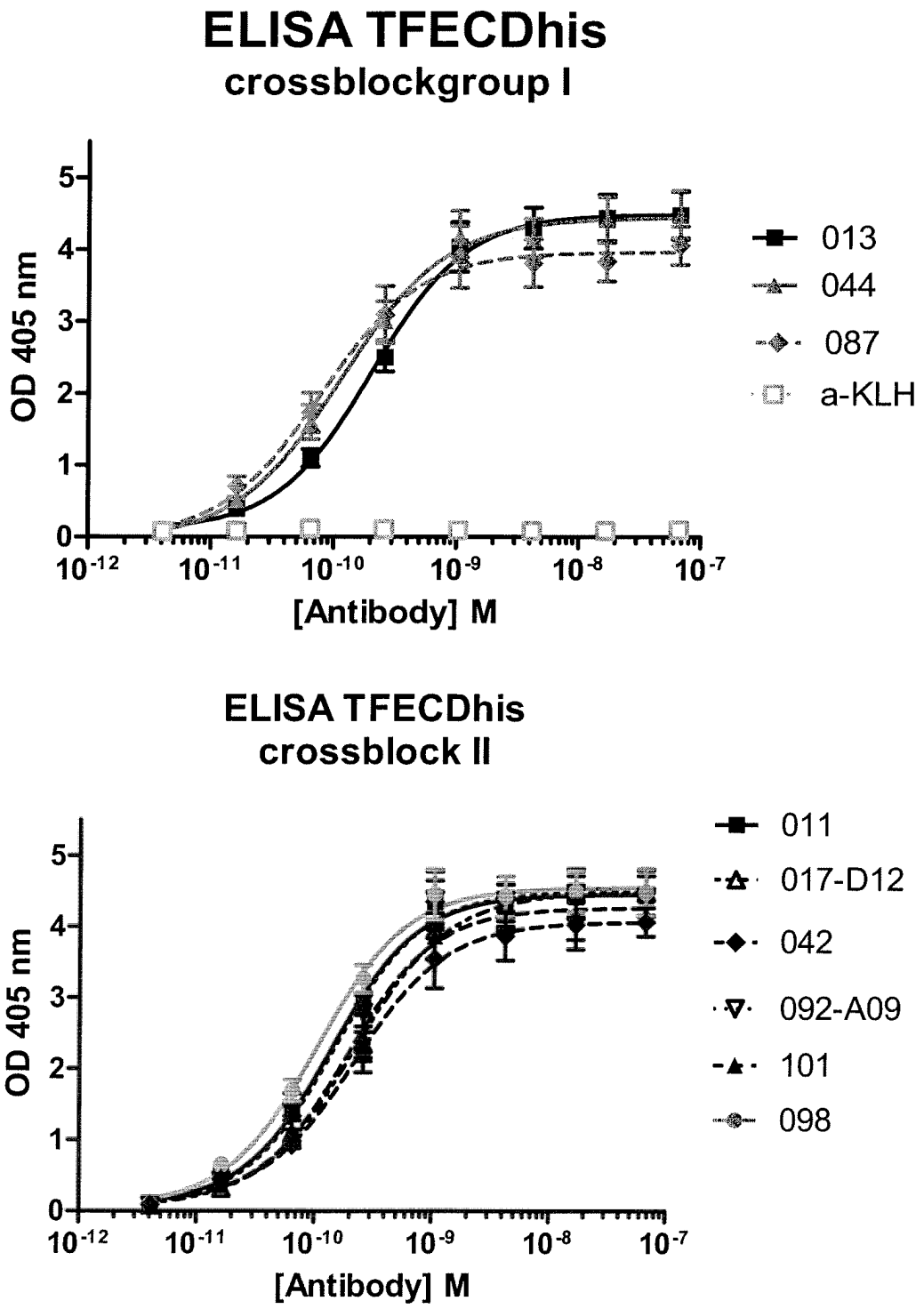

ELISA TFECDhis
crossblockgroup I
OD 405 nm
0
1
2
3
4
5
10-12
10-11
10-10
10-9
10-8
10-7
[Antibody] M
013
044
087
a-KLH
ELISA TFECDhis
crossblock II
OD 405 nm
0
1
2
3
4
5
10-12
10-11
10-10
10-9
10-8
10-7
[Antibody] M
011
017-D12
042
092-A09
101
098

Figure 3 continued...

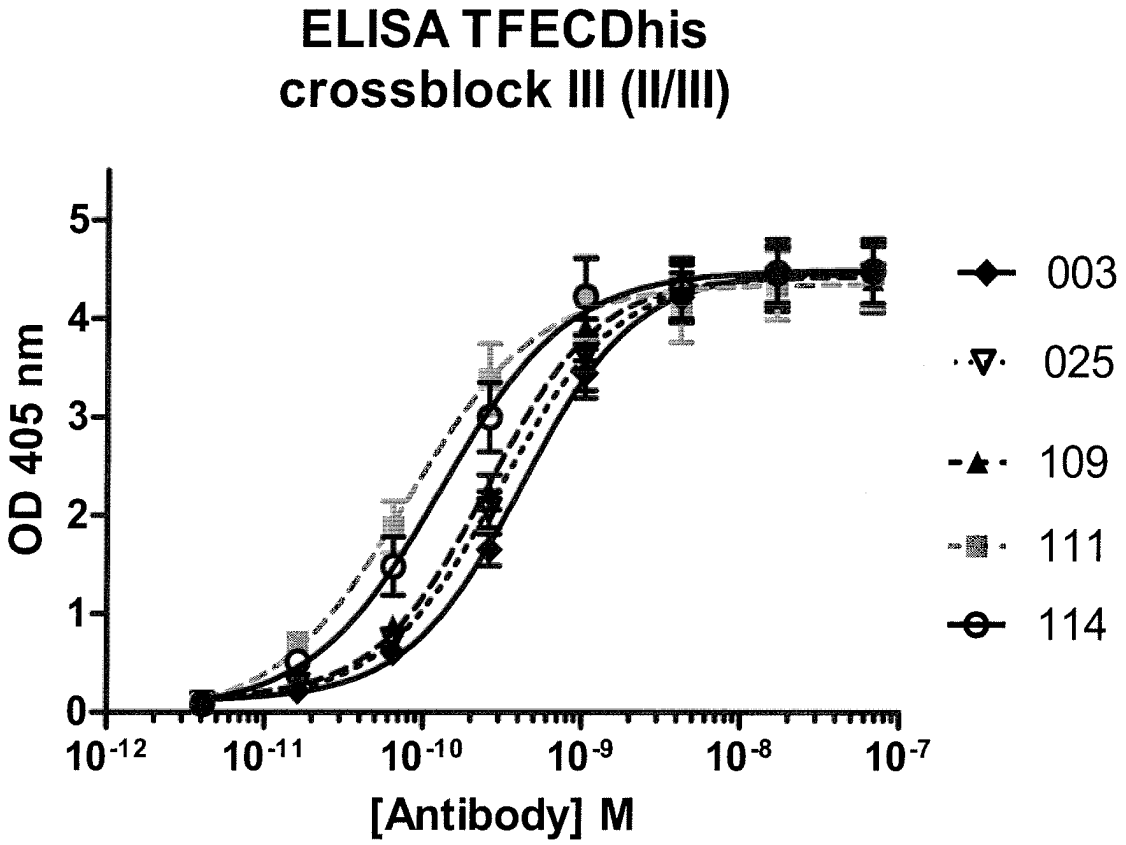
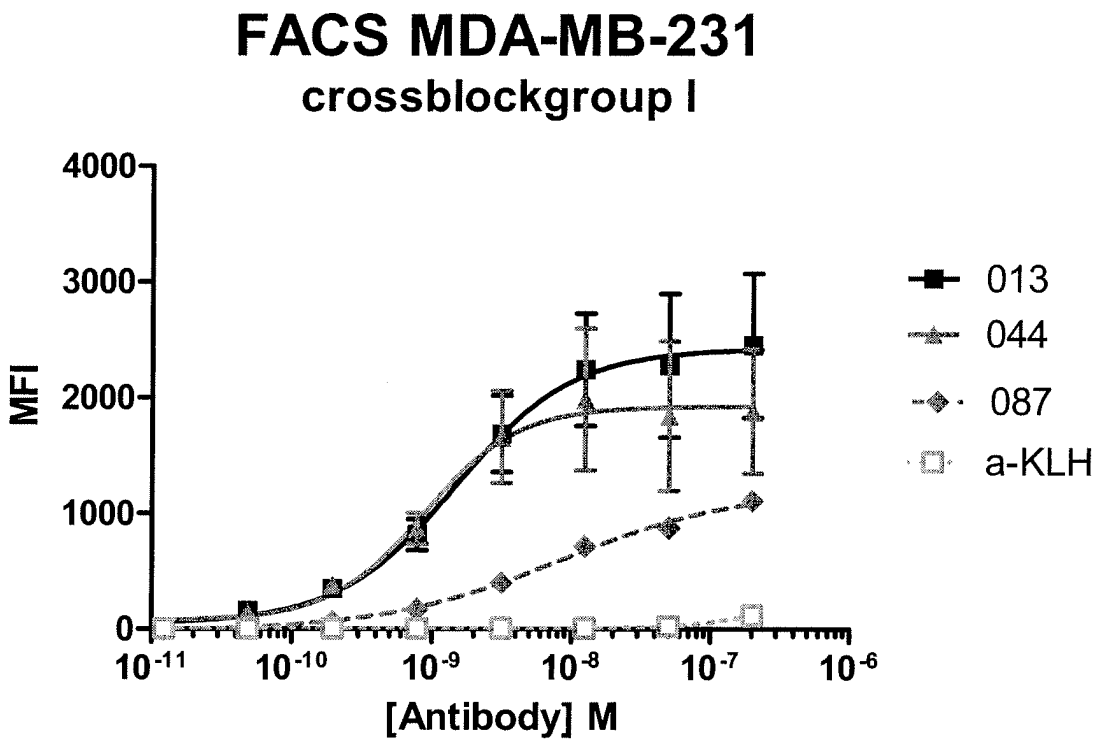


Figure 3: Binding of anti-TF HuMabs to the extra cellular domain of TF in ELISA_Binding was determined by ELISA.

Figure 4


FACS MDA-MB-231
crossblockgroup I
MFI
4000
3000
2000
1000
0
10-11
10-10
10-9
10-8
10-7
10-6
[Antibody] M
013
044
087
a-KLH

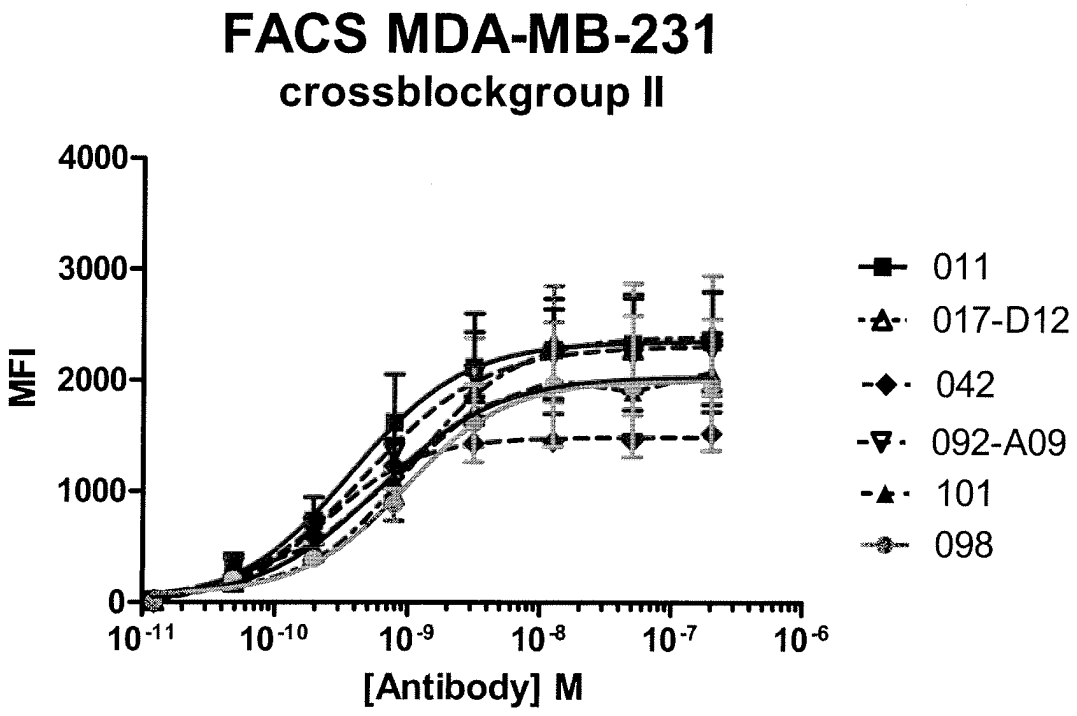

FACS MDA-MB-231
crossblockgroup II
MFI
4000
3000
2000
1000
0
10-11
10-10
10-9
10-8
10-7
10-6
[Antibody] M
011
017-D12
042
092-A09
101
098

Figure 4 continued

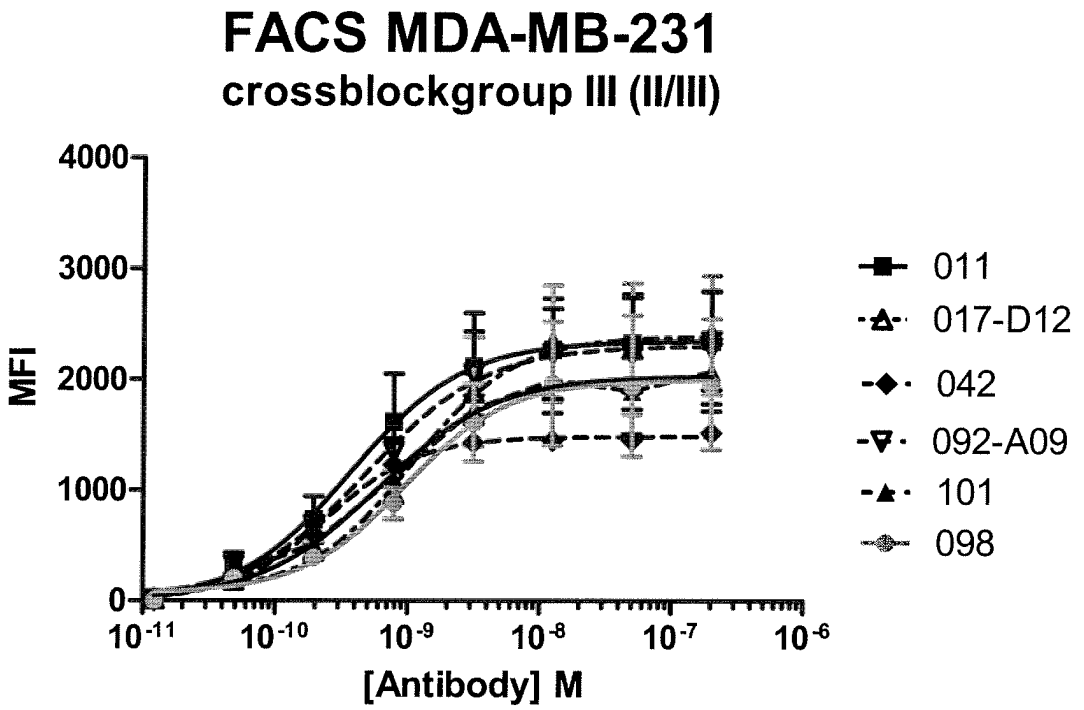
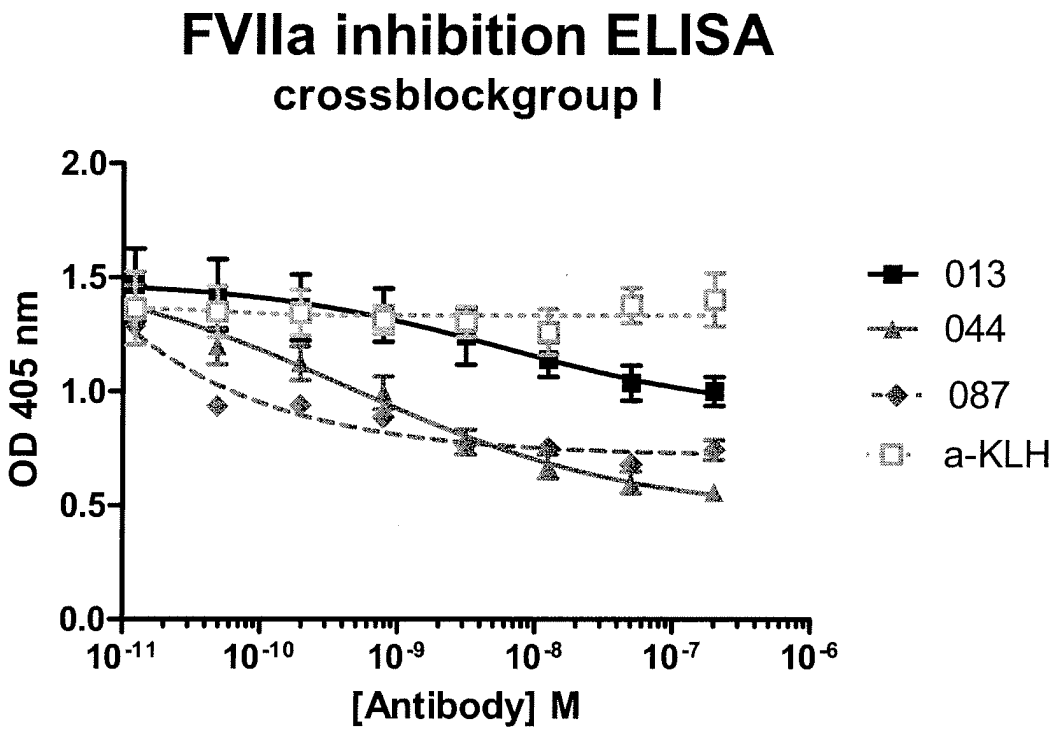


Figure 4a, 4b, 4c: Binding of anti-TF HuMabs to membrane-bound TF on MDA-MD-231 cells. Binding was determined by FACS analysis.

Figure 5


FVIIa inhibition ELISA
crossblockgroup I
OD 405 nm
2.0
1.5
1.0
0.5
0.0
10-11
10-10
10-9
10-8
10-7
10-6
[Antibody] M
013
044
087
a-KLH

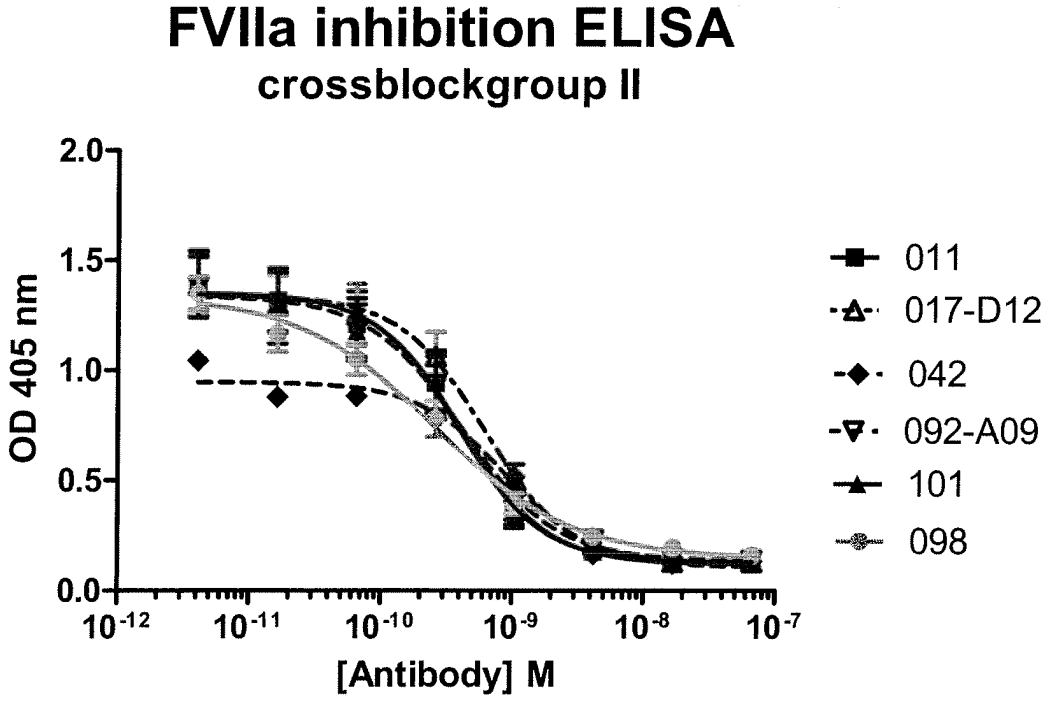

FVIIa inhibition ELISA
crossblockgroup II
OD 405 nm
2.0
1.5
1.0
0.5
0.0
10-12
10-11
10-10
10-9
10-8
10-7
[Antibody] M
011
017-D12
042
092-A09
101
098

Figure 5 continued...

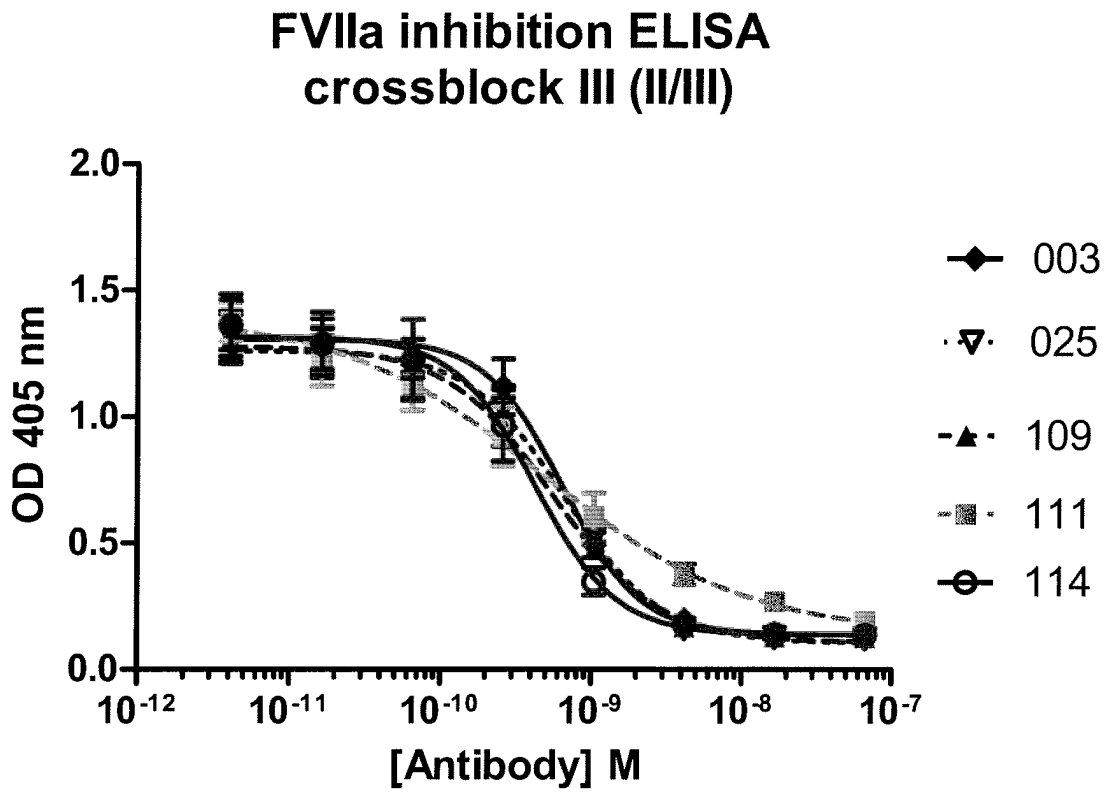
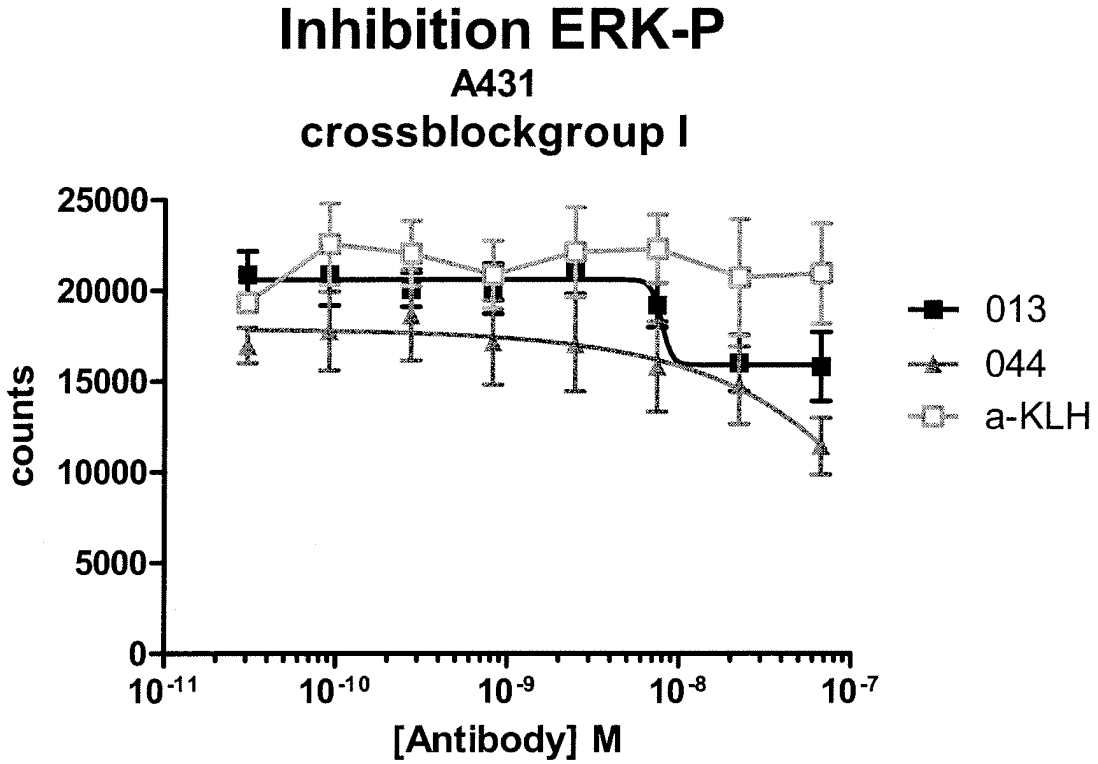


Figure 5: **Inhibition of FVIIa binding to TF.** FVIIa binding, and the inhibition by TF specific HuMabs of this binding, was measured by ELISA.

Figure 6


Inhibition ERK-P
A431
crossblockgroup I
25000
20000
15000
10000
5000
0
counts
10-11
10-10
10-9
10-8
10-7
[Antibody] M
013
044
a-KLH

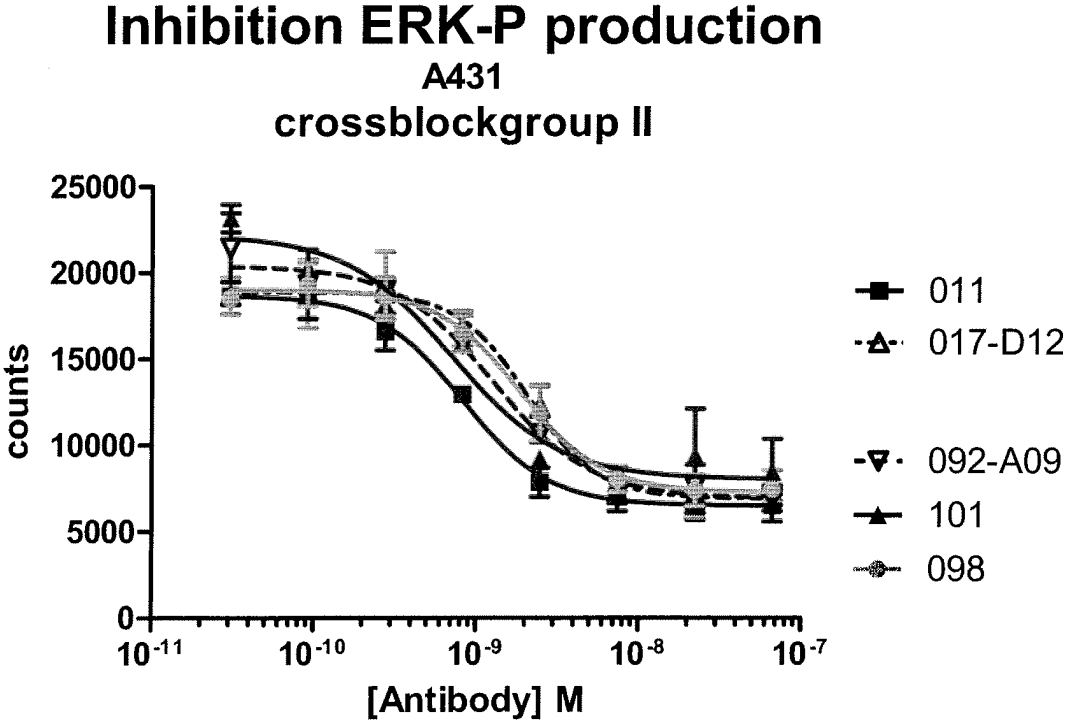

Inhibition ERK-P production
A431
crossblockgroup II
25000
20000
15000
10000
5000
0
counts
10-11
10-10
10-9
10-8
10-7
[Antibody] M
011
017-D12
092-A09
101
098

Figure 6 continued...

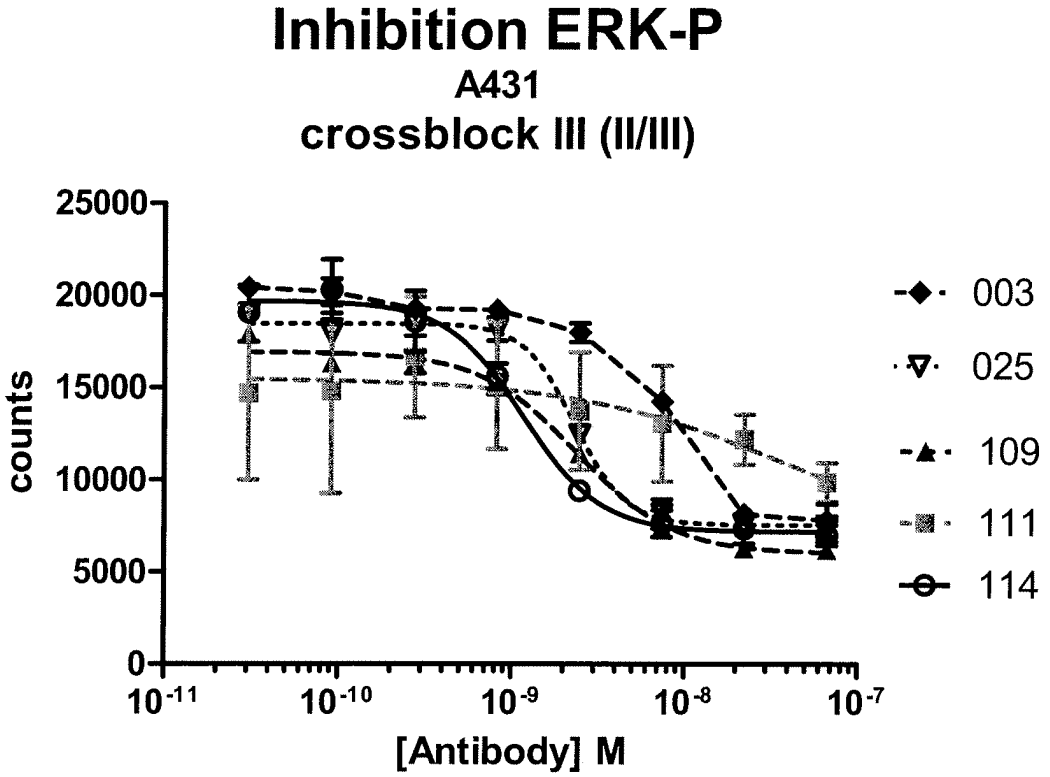


Figure 6: Inhibition of FVIIa induced ERK phosphorylation.

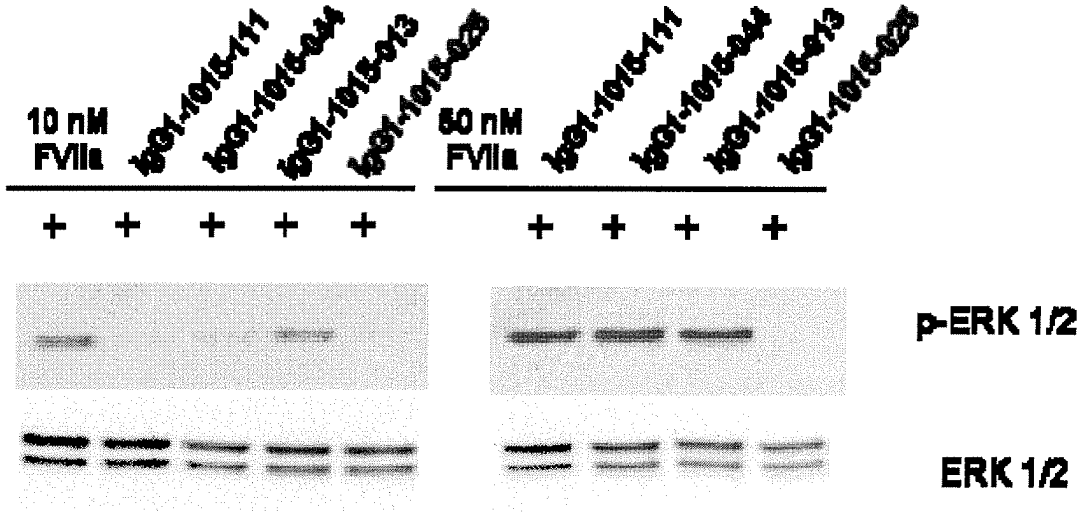


Figure 6A. Inhibition of FVIIa induced ERK phosphorylation, using Western blot analysis.

Figure 7

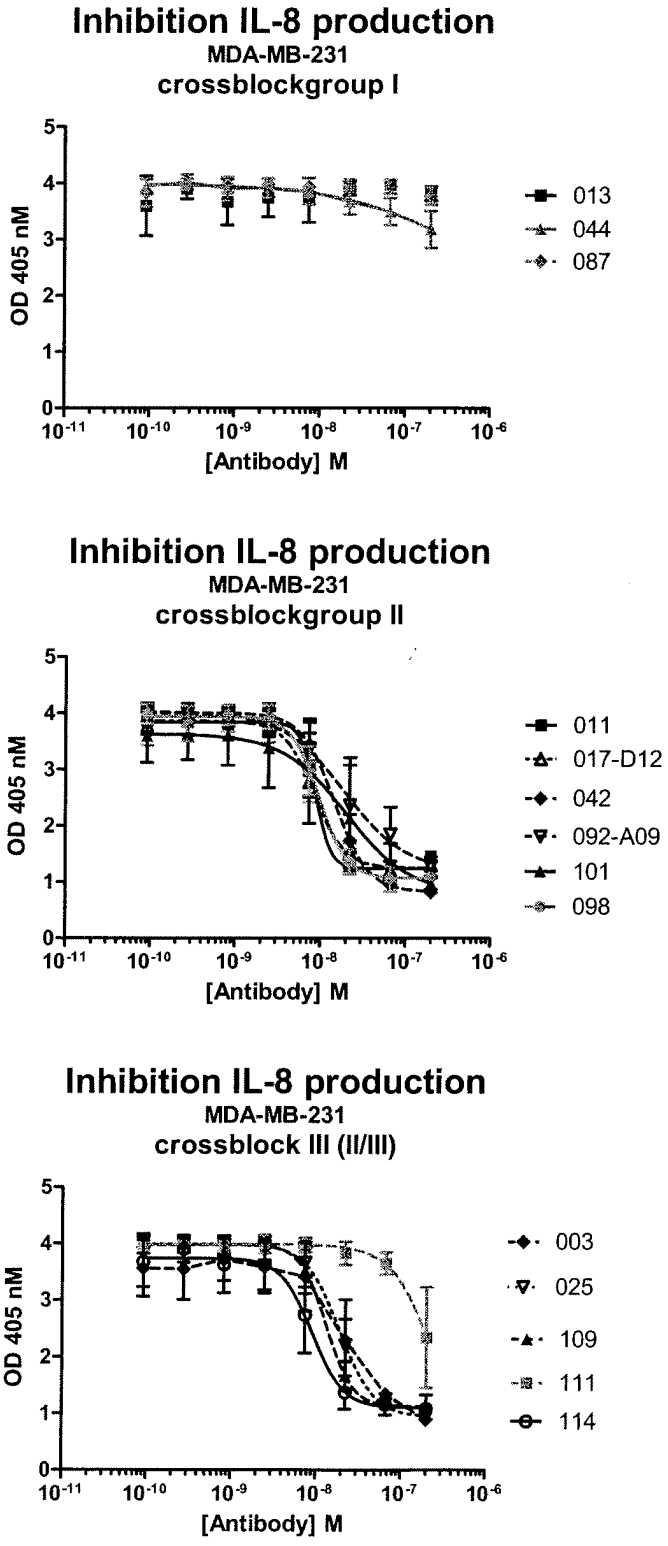
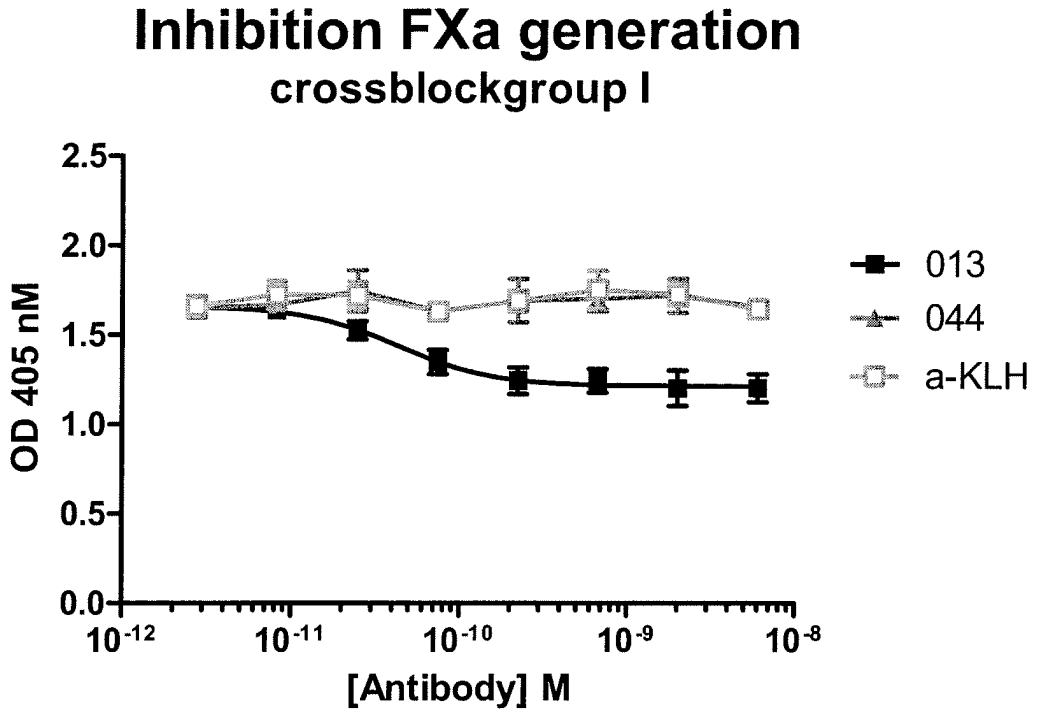

Inhibition IL-8 production
MDA-MB-231
crossblockgroup I
OD 405 nM
[Antibody] M
013
044
087
Inhibition IL-8 production
MDA-MB-231
crossblockgroup II
OD 405 nM
[Antibody] M
011
017-D12
042
092-A09
101
098
Inhibition IL-8 production
MDA-MB-231
crossblock III (II/III)
OD 405 nM
[Antibody] M
003
025
109
111
114

Figure 7 continued...

Figure 7. Inhibition of FVIIa induced IL-8 release. MDA-MB-231 were cultured in serum free medium, TF specific antibodies and FVIIa were added. FVIIa induced IL-8 was measured by ELISA.

Figure 8


Inhibition FXa generation
crossblockgroup I
OD 405 nM
2.5
2.0
1.5
1.0
0.5
0.0
10-12
10-11
10-10
10-9
10-8
[Antibody] M
013
044
a-KLH

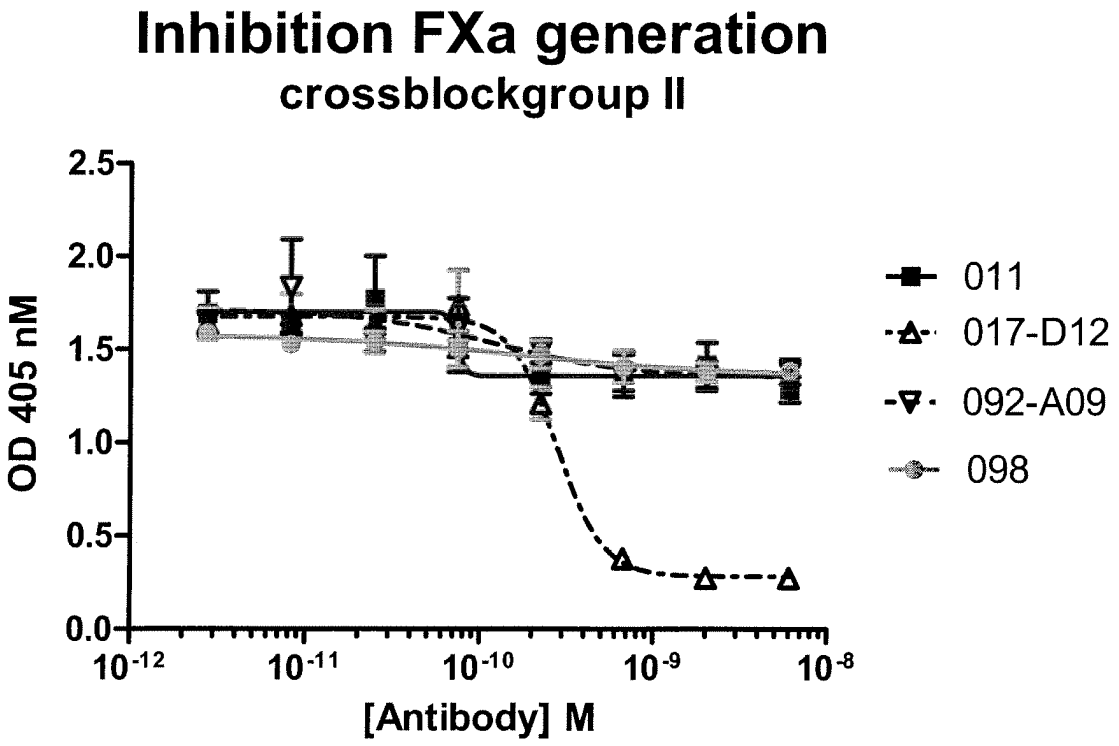

Inhibition FXa generation
crossblockgroup II
OD 405 nM
2.5
2.0
1.5
1.0
0.5
0.0
10-12
10-11
10-10
10-9
10-8
[Antibody] M
011
017-D12
092-A09
098

Figure 8 continued...

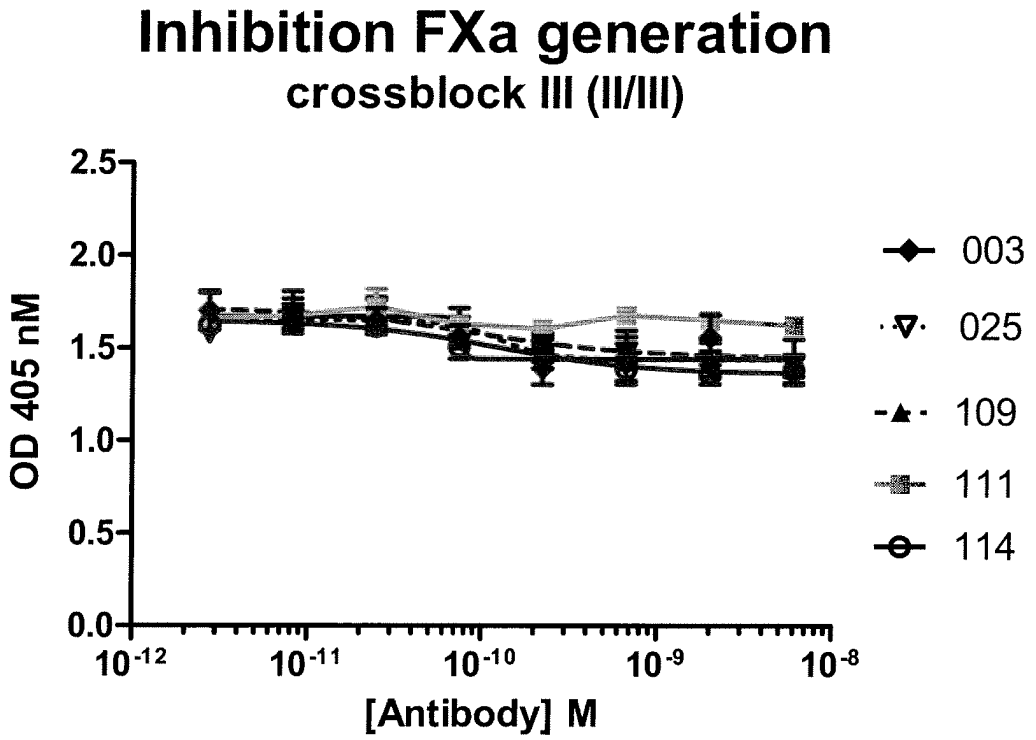
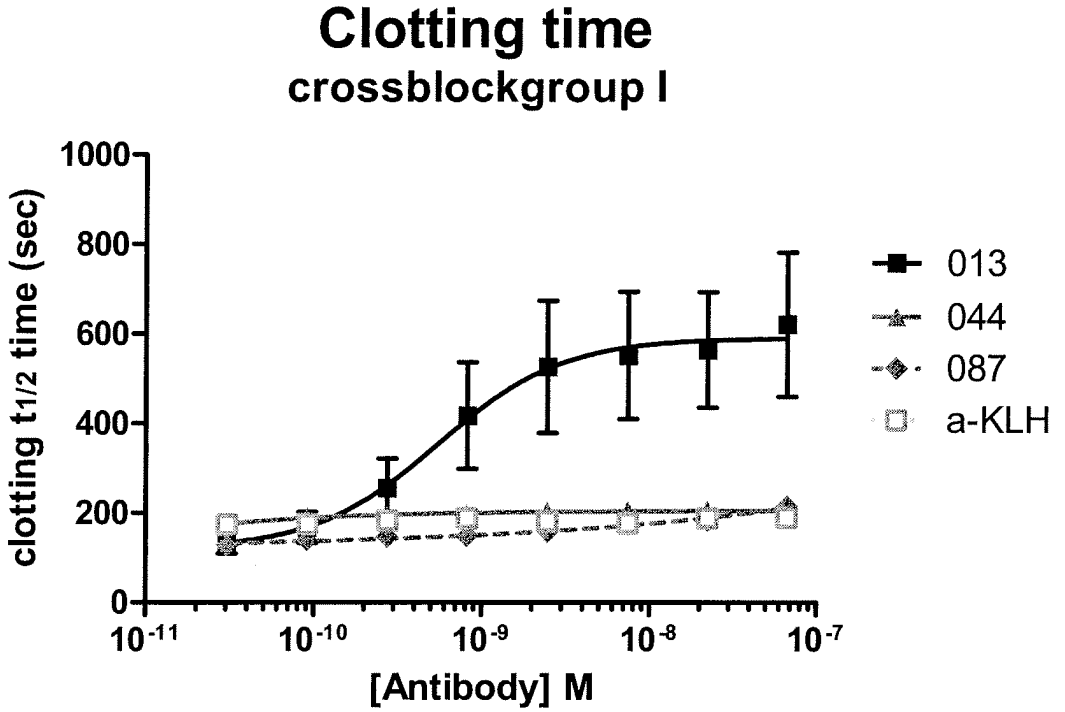


Figure 8. Inhibition of FXa generation. The ability of TF specific HuMabs to inhibit FXa generation was tested in an assay in which conversion of FX into FXa by the TF/FVIIa complex is measured using a colometric FXa specific substrate.

Figure 9


Clotting time
crossblockgroup I
clotting t1/2 time (sec)
1000
800
600
400
200
0
10-11
10-10
10-9
10-8
10-7
[Antibody] M
013
044
087
a-KLH

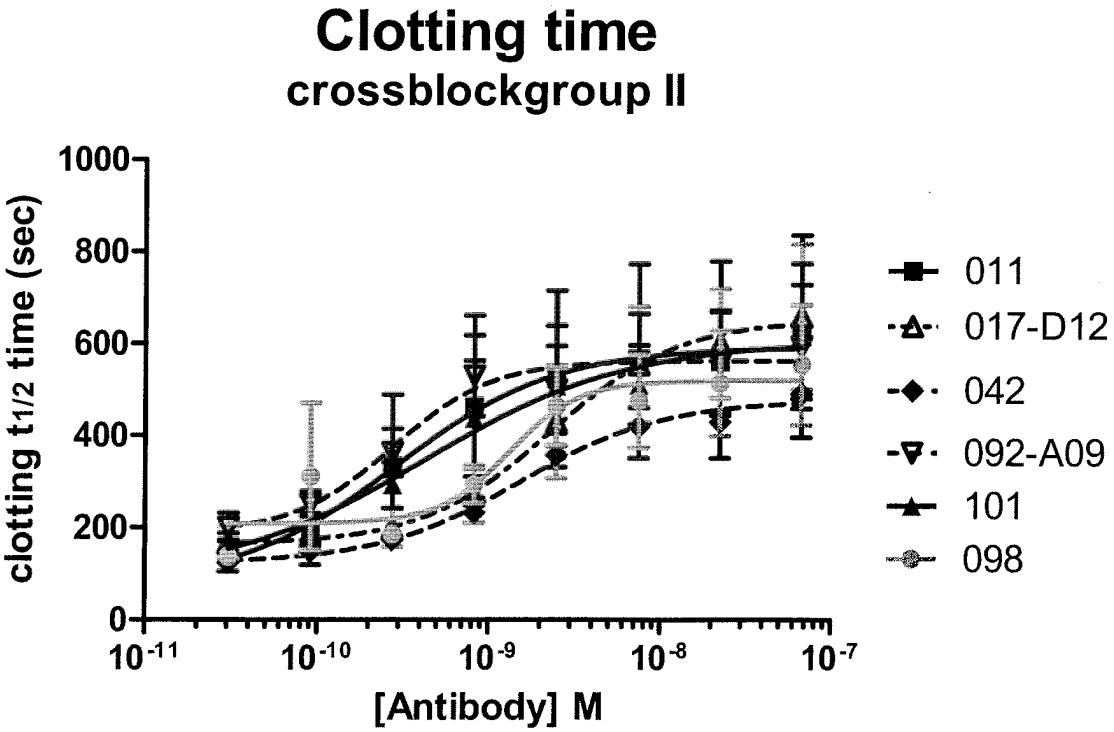

Clotting time
crossblockgroup II
clotting t1/2 time (sec)
1000
800
600
400
200
0
10-11
10-10
10-9
10-8
10-7
[Antibody] M
011
017-D12
042
092-A09
101
098

Figure 9 continued...

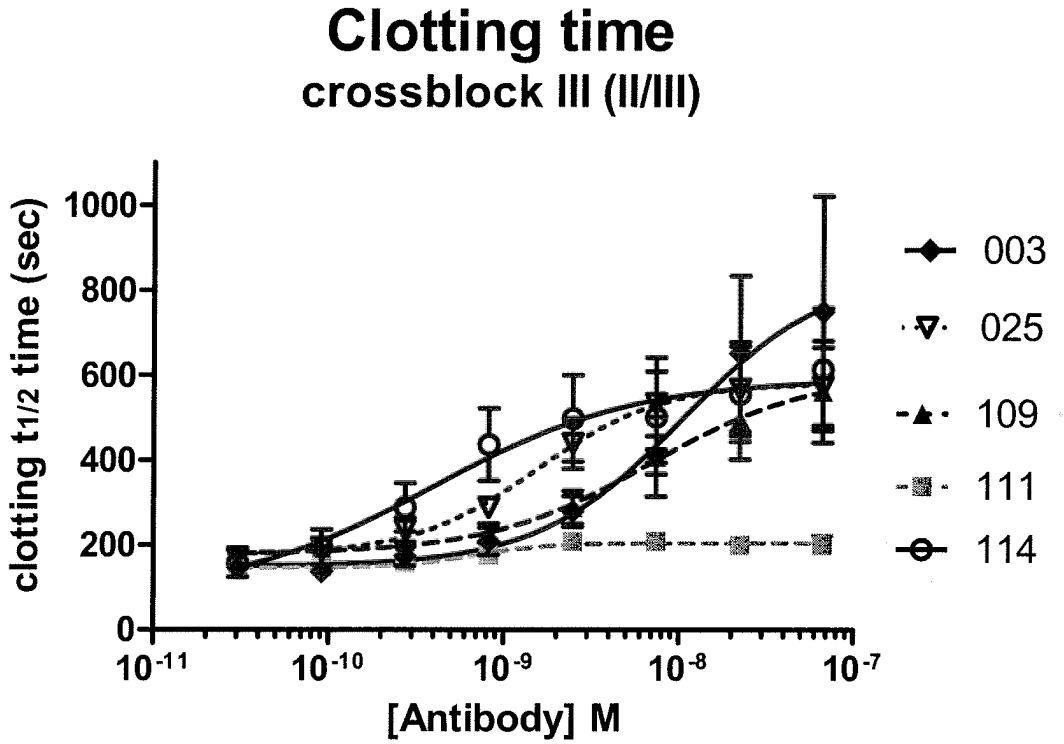
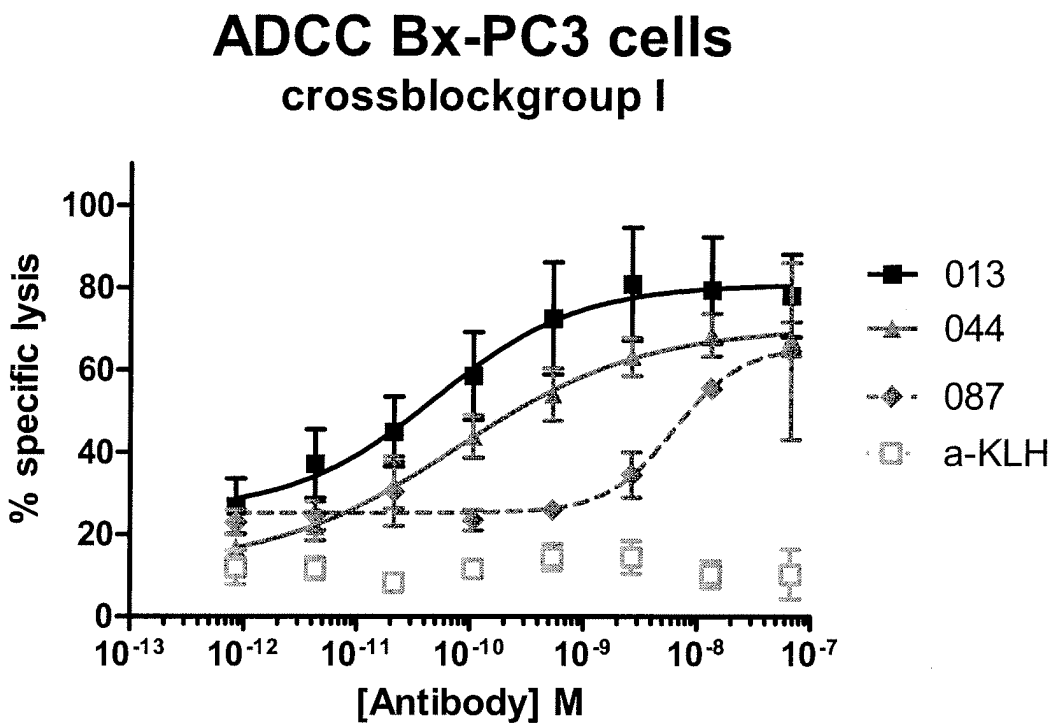


Figure 9. Inhibition of blood coagulation. Inhibition of blood coagulation by TF-HuMabs was measured in an assay determining TF induced clotting time.

Figure 10


ADCC Bx-PC3 cells
crossblockgroup I
% specific lysis
100
80
60
40
20
0
10-13
10-12
10-11
10-10
10-9
10-8
10-7
[Antibody] M
013
044
087
a-KLH

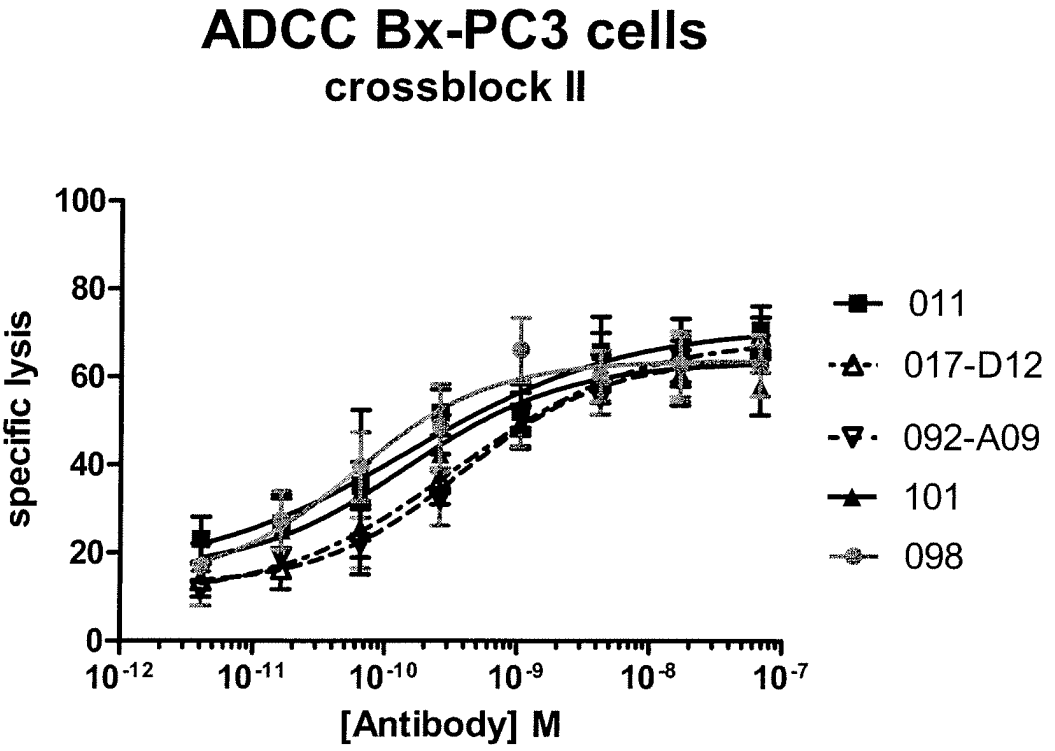

ADCC Bx-PC3 cells
crossblock II
specific lysis
100
80
60
40
20
0
10-12
10-11
10-10
10-9
10-8
10-7
[Antibody] M
011
017-D12
092-A09
101
098

Figure 10 continued...

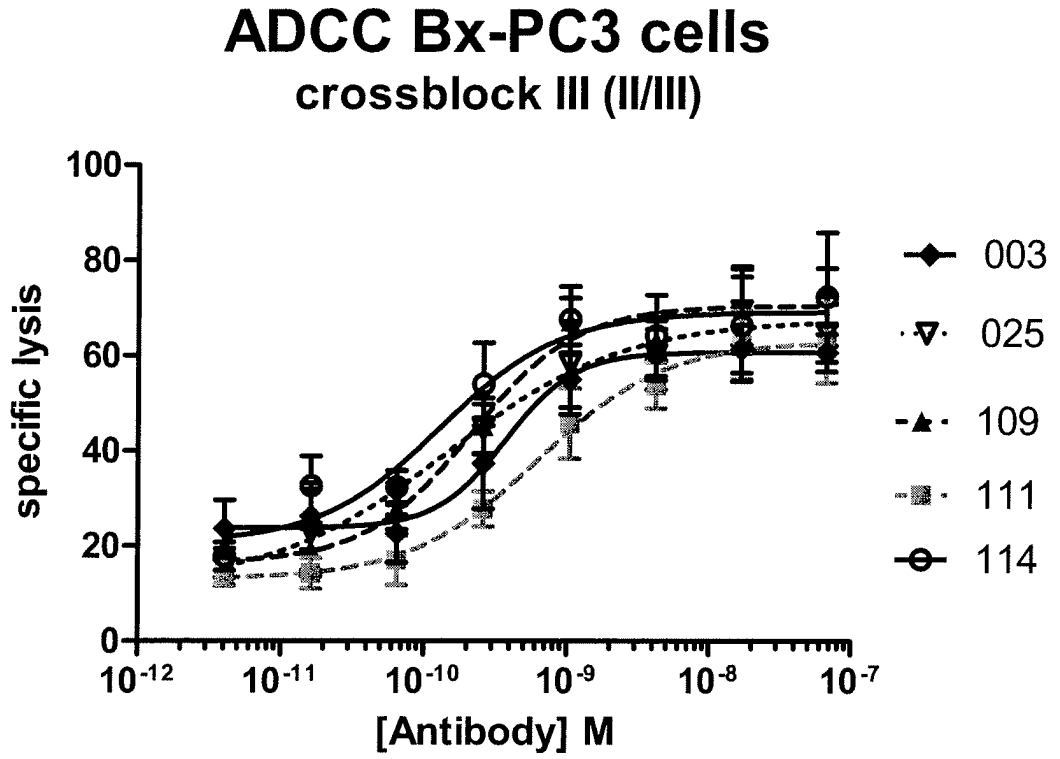


Figure 10: TF-HuMabs induced lysis of Bx-PC3 cells by ADCC.

Figure 11

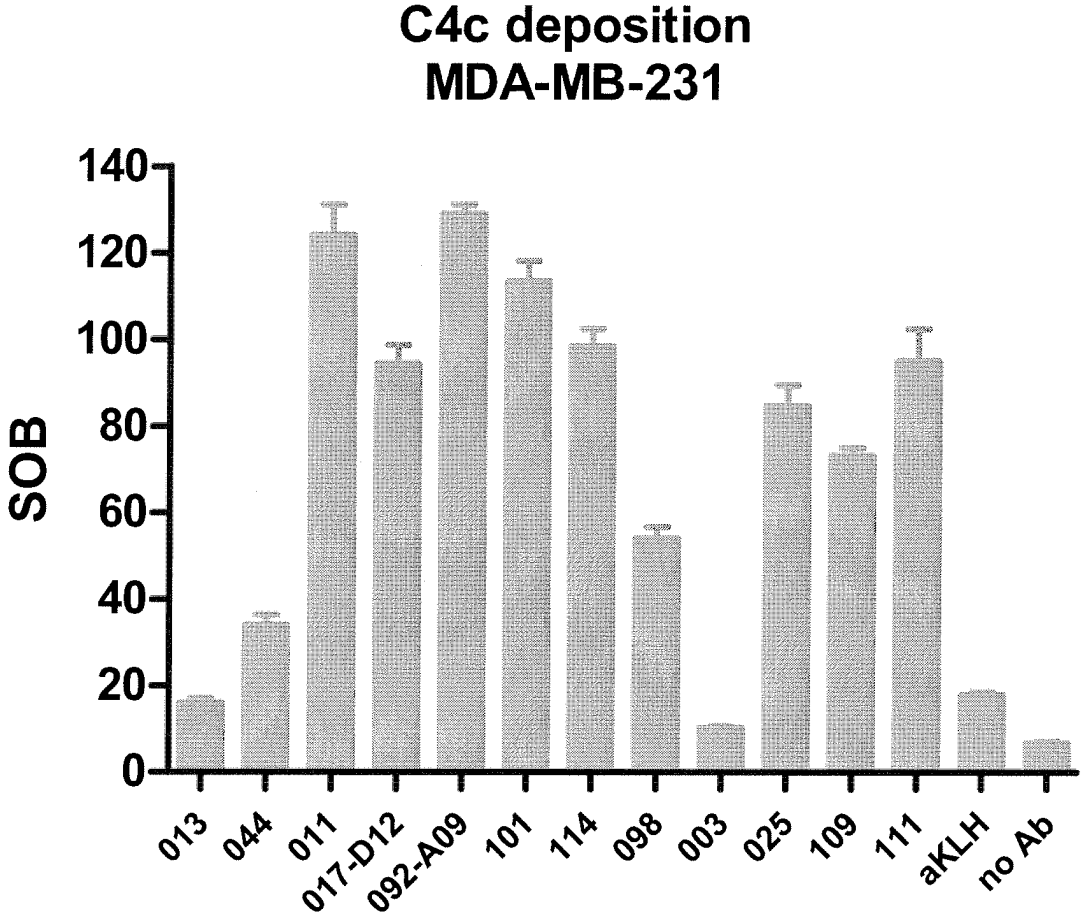

C4c deposition
MDA-MB-231
SOB
140
120
100
80
60
40
20
0
013
044
011
017-D12
092-A09
101
114
098
003
025
109
111
aKLH
no Ab

Figure 11 continued...

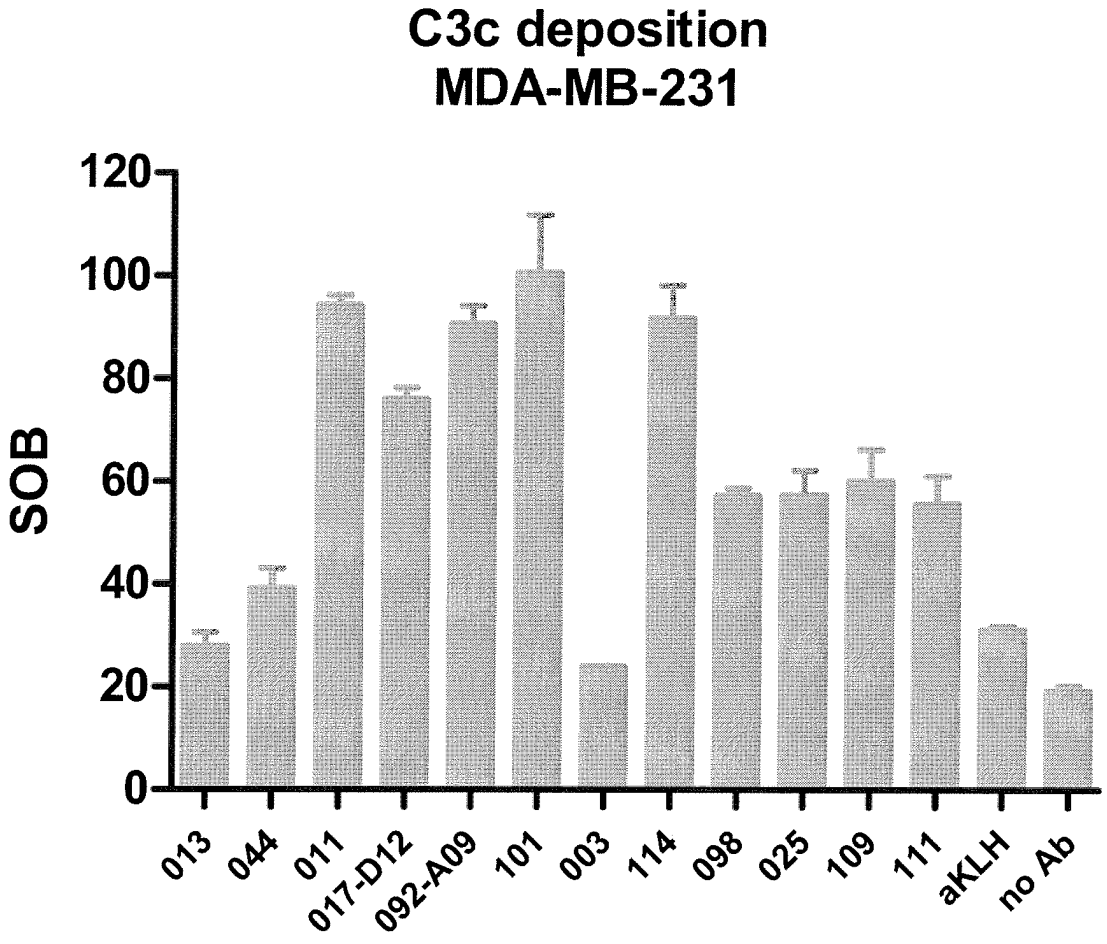


Figure 11 continued...

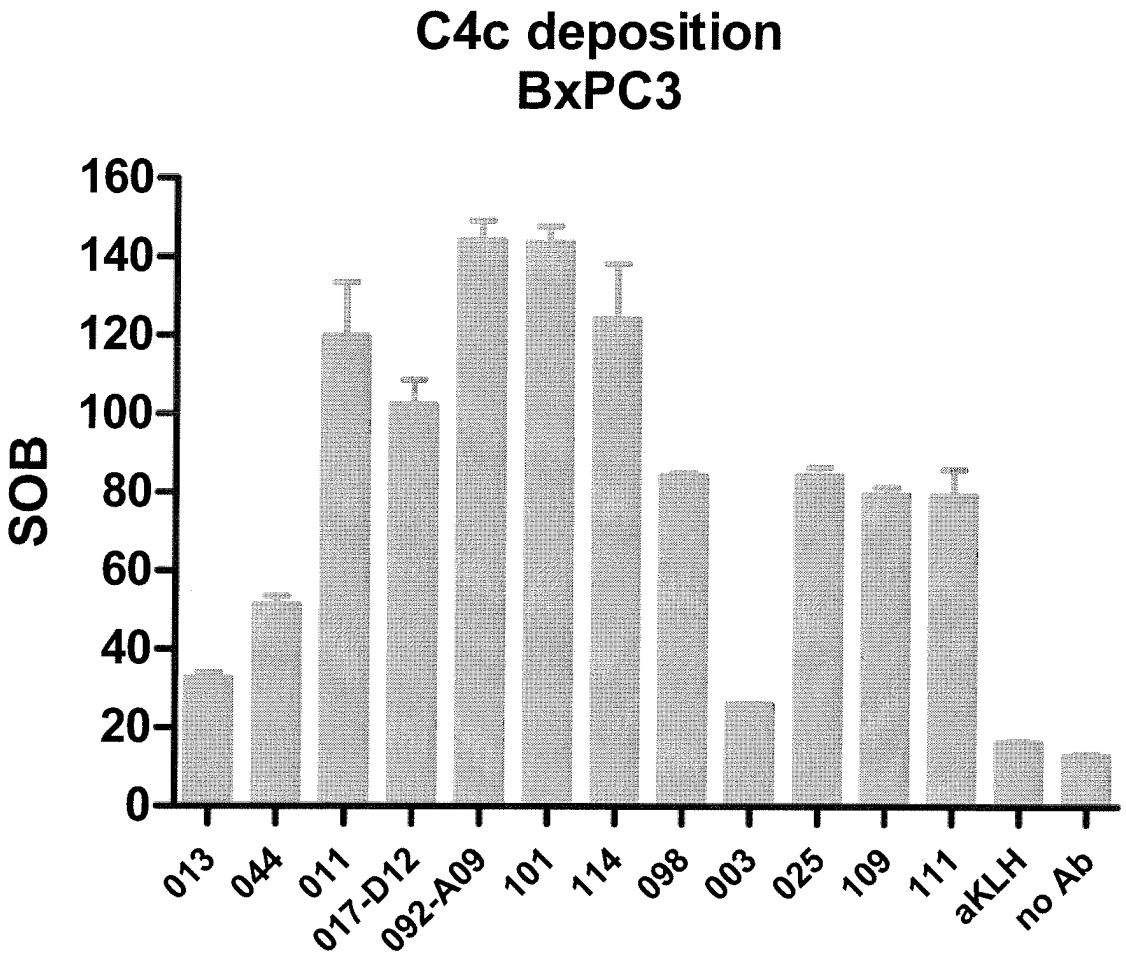


Figure 11 continued...

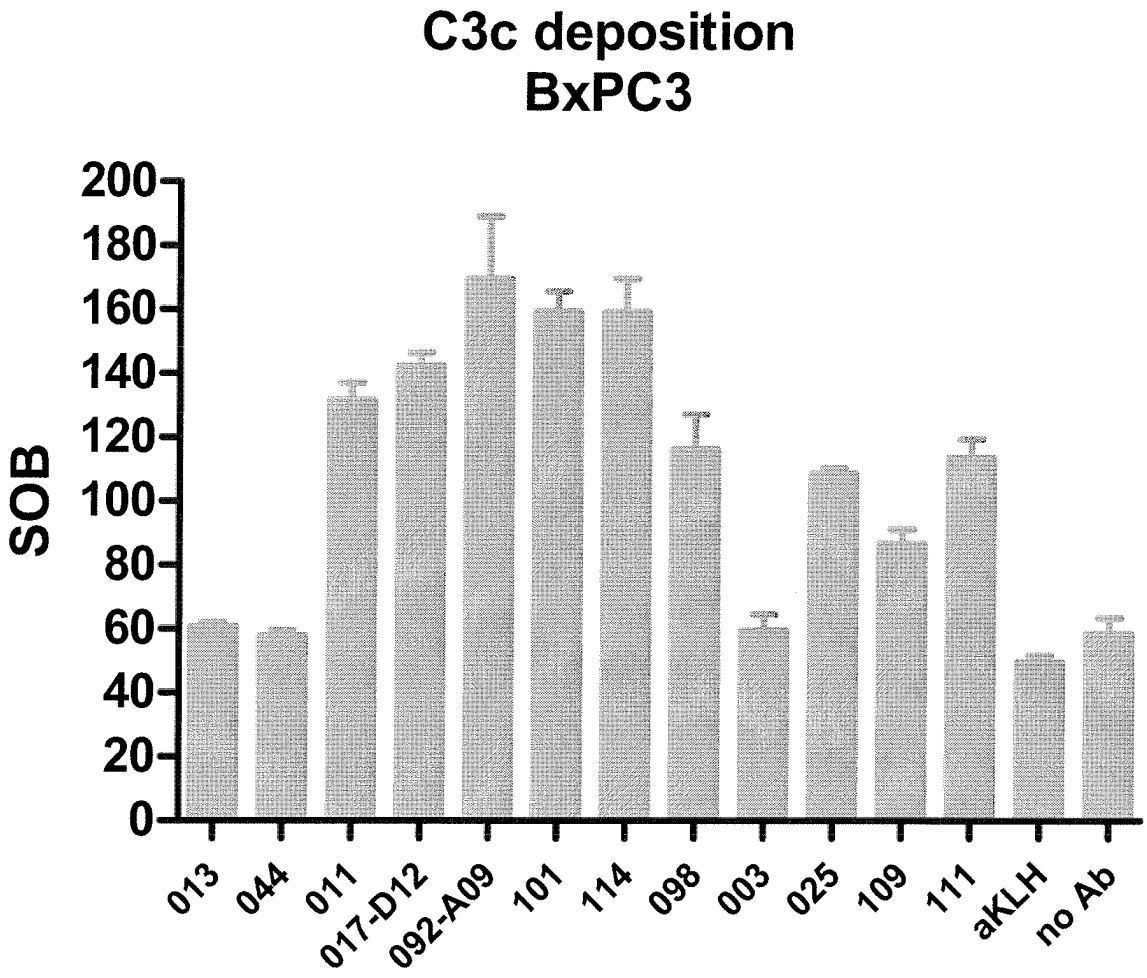


Figure 11: Complement deposition

Figure 12

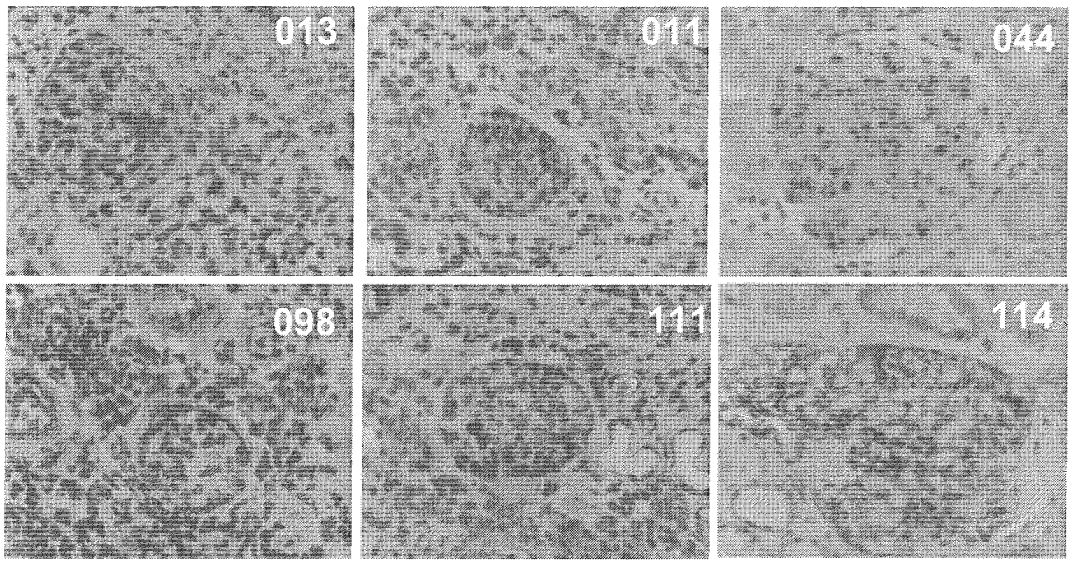


Figure 12: Immunohistochemical analysis of binding of TF-HuMabs to normal human kidney.

Figure 13

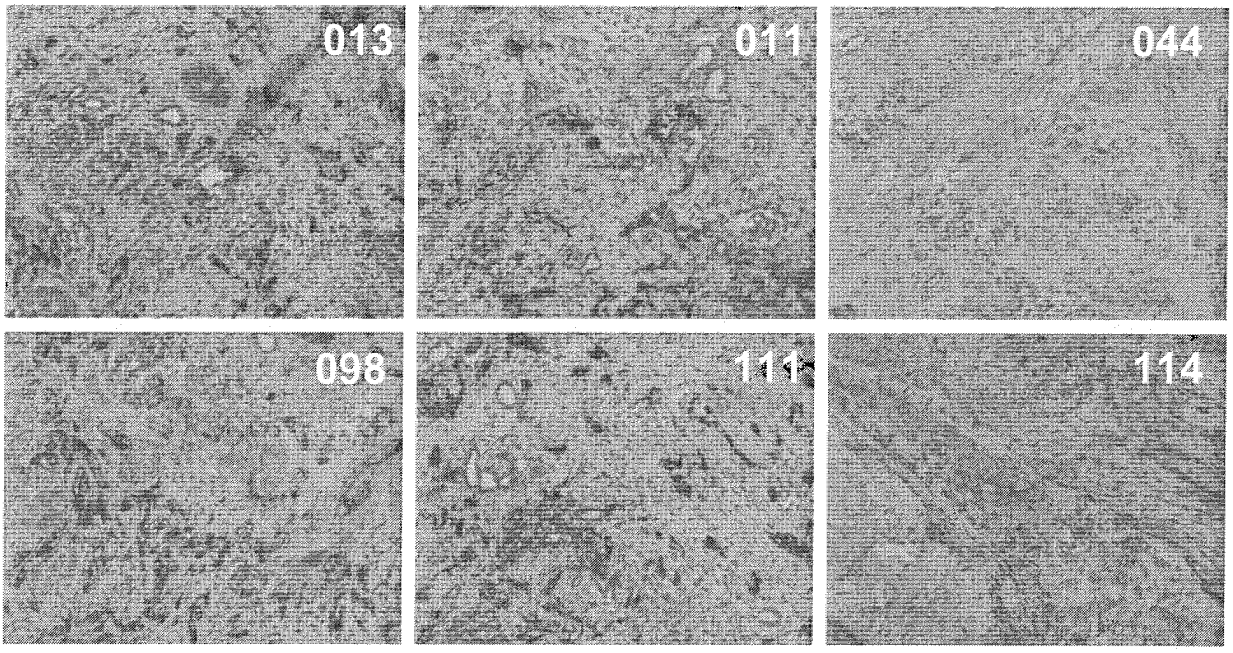


Figure 13. Immunohistochemical analysis of binding of TF-HuMabs to pancreatic tumors.

Figure 14

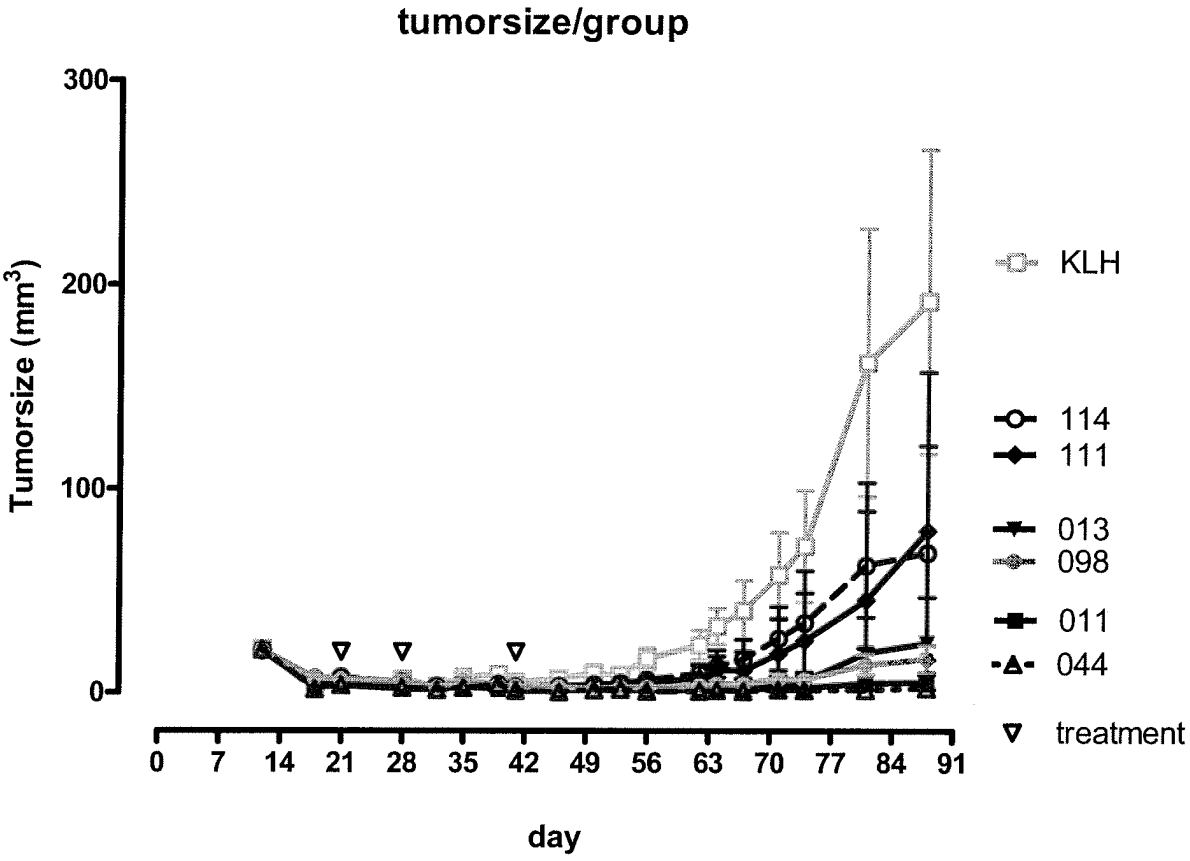

tumorsize/group
Tumorsize (mm3)
300
200
100
0
0 7 14 21 28 35 42 49 56 63 70 77 84 91
day
KLH
114
111
013
098
011
044
treatment

Figure 14 continued...

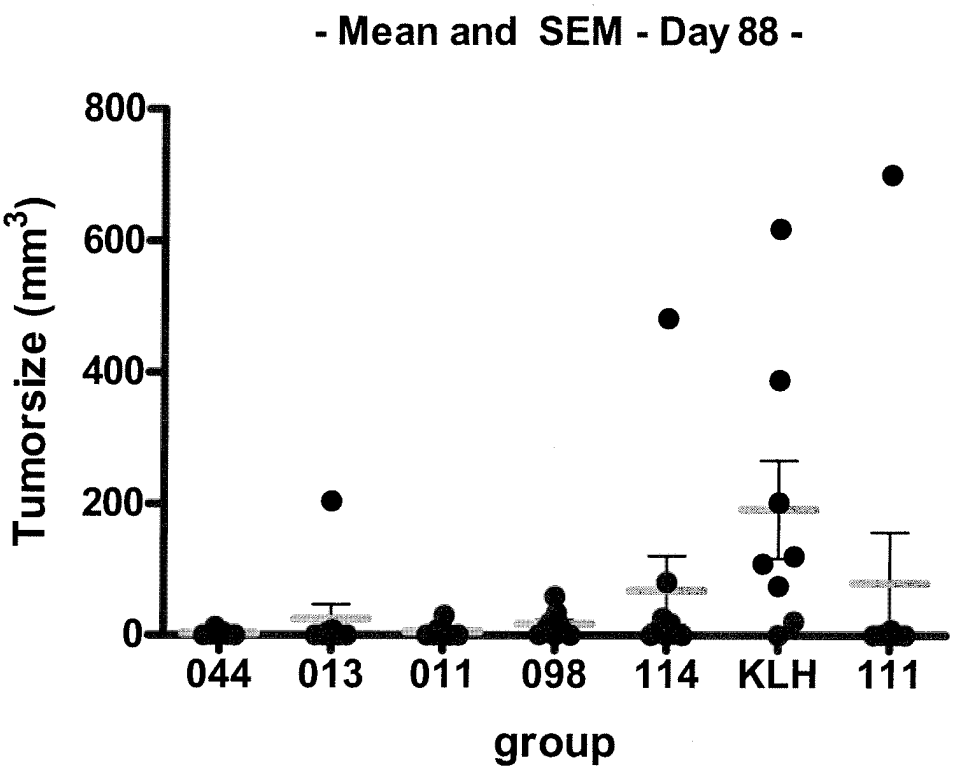


Figure 14. In vivo efficacy of TF-HuMabs in established MDA-MB-231 tumor xenograft in mammary fat pads of SCID mice.

Figure 15

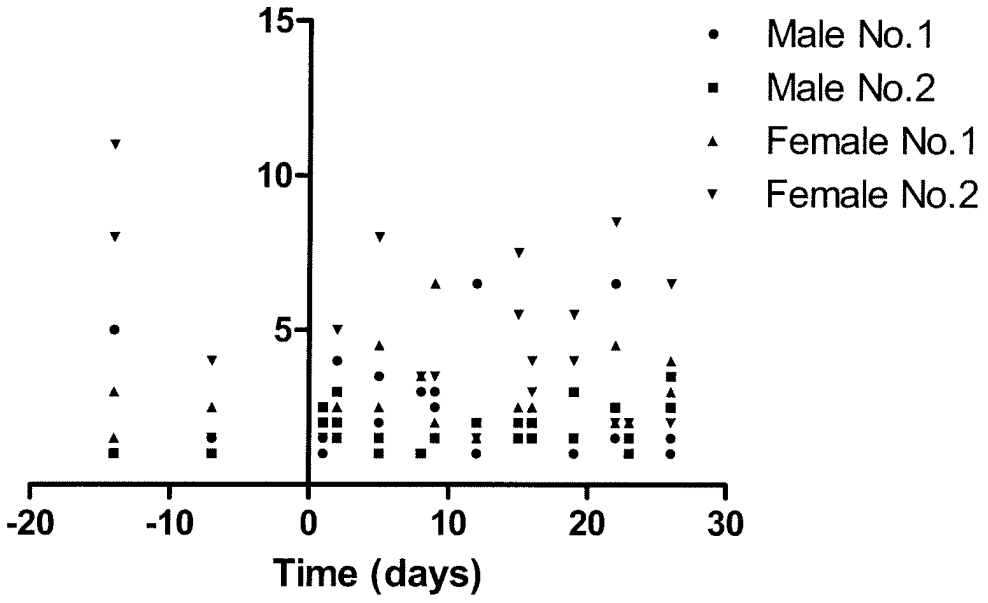
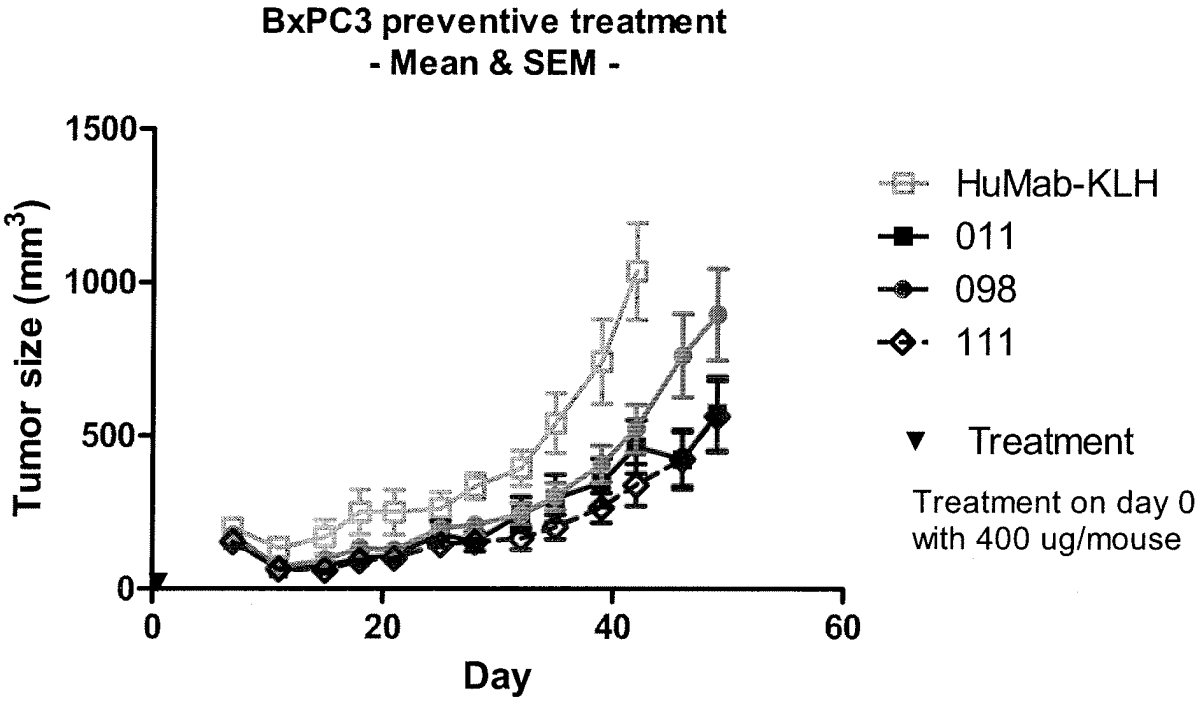
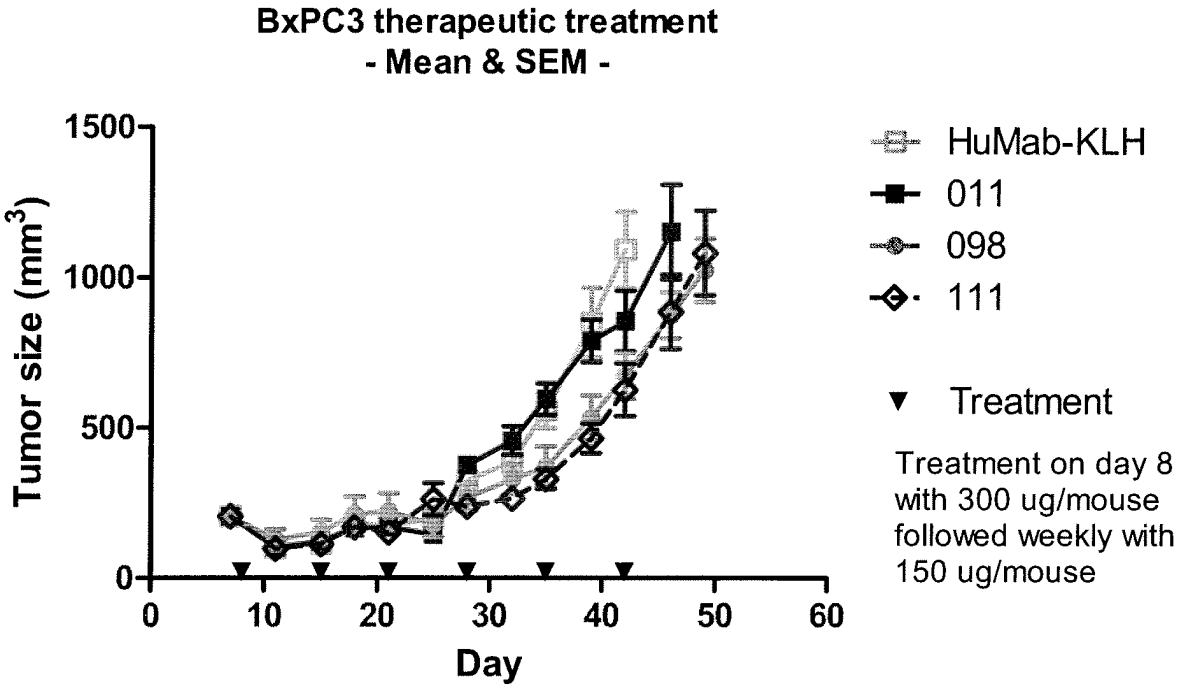


Figure 15: Bleeding time (minutes), determined in cynomolgus monkeys upon intravenous injections of TF-specific HuMab 011. The antibody was administered on day 1 (0 mg/kg), 8 (1 mg/kg), 15 (10 mg/kg) and 22 (100 mg/kg). Functional bleeding time and blood loss was determined 1, 24 and 120 hours post dosing

Figure 16



Repeated measures 2-way ANOVA, followed by Bonferroni posthoc testing:
111 vs KLH: from d28 onwards: $P<0.05$, from d32 onwards: $P<0.01$.



Repeated measures 2-way ANOVA, followed by Bonferroni posthoc testing:

111 vs KLH: from d35 onwards: $P<0.05$

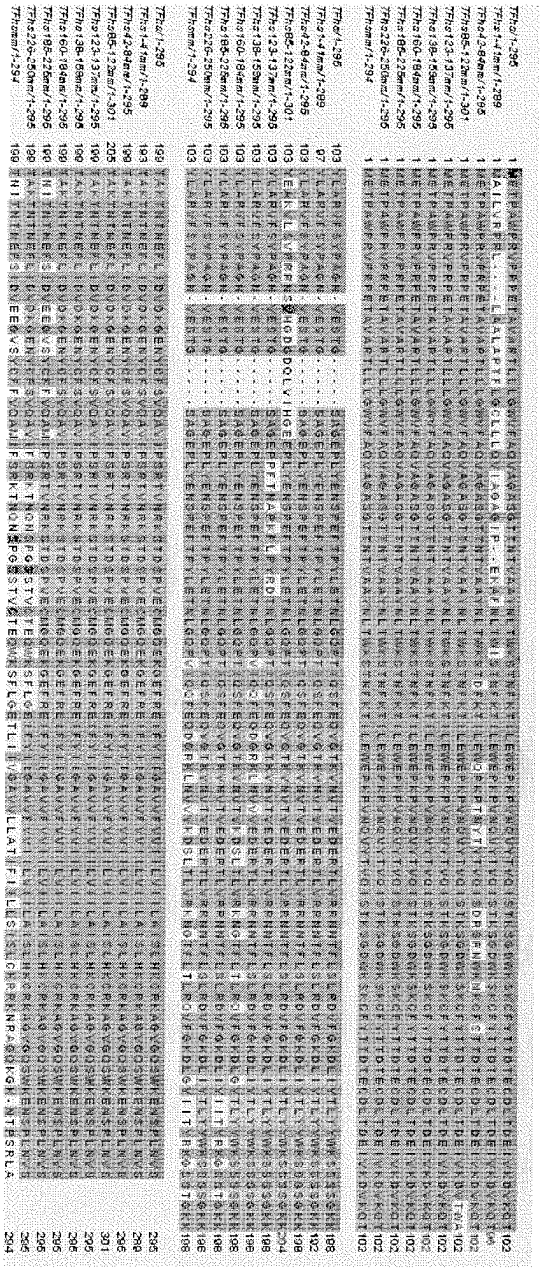


Figure 17 A. TFhs shuffle construct, containing TFmm domains

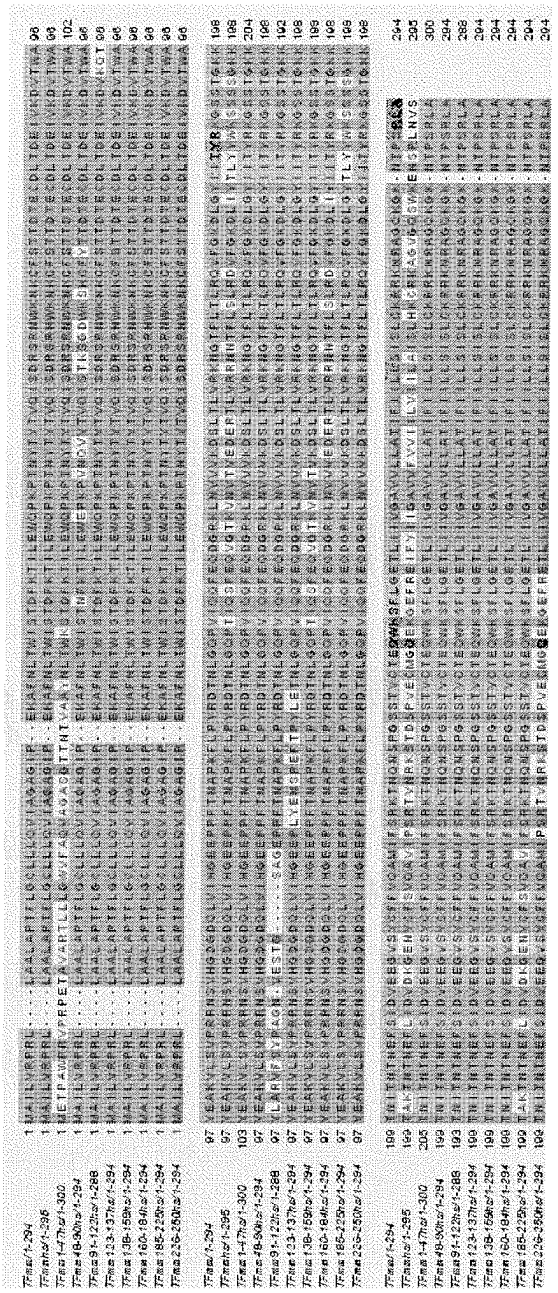


Figure 17 B. TFmm shuffle construct, containing TFhs domains

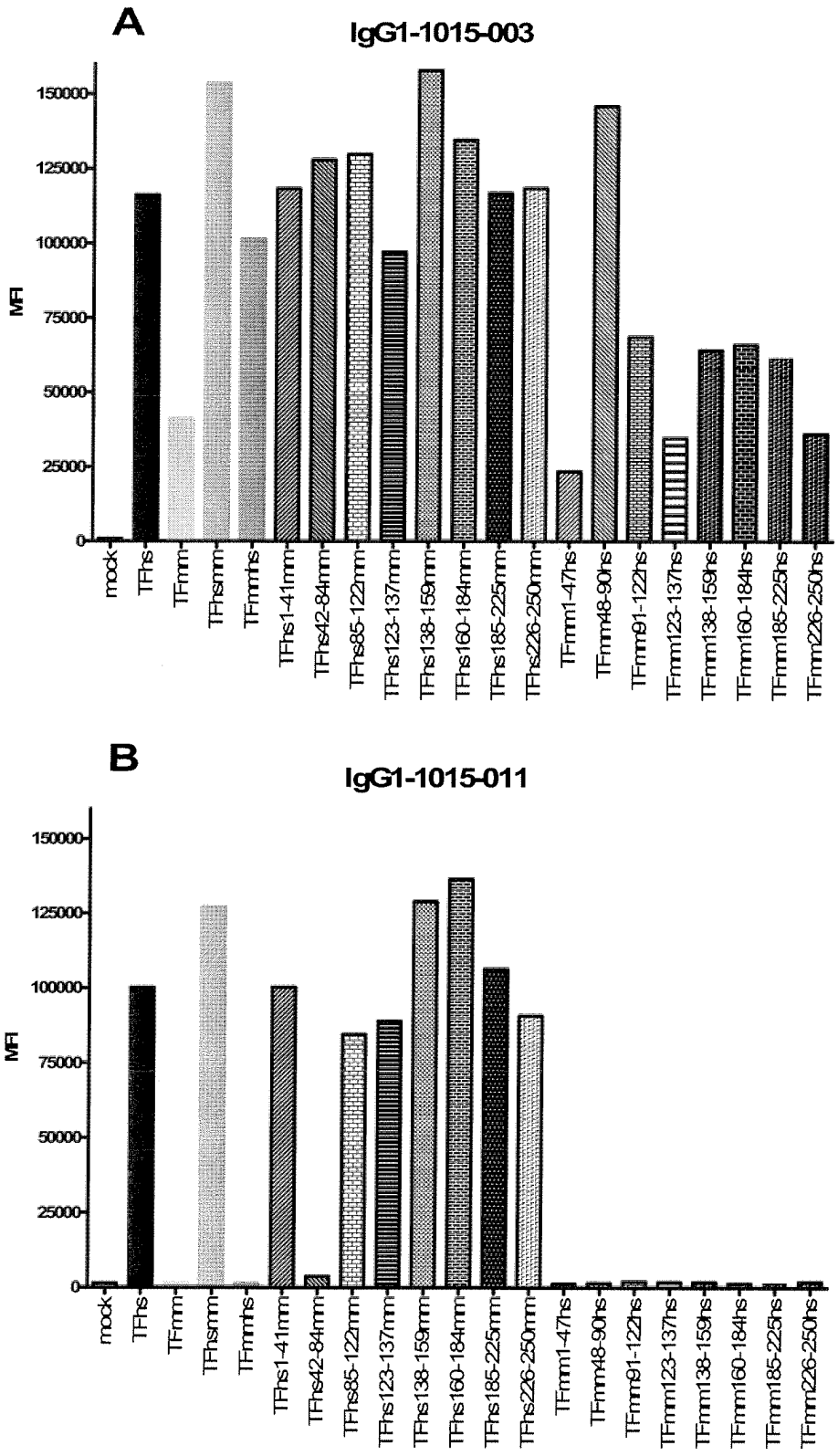
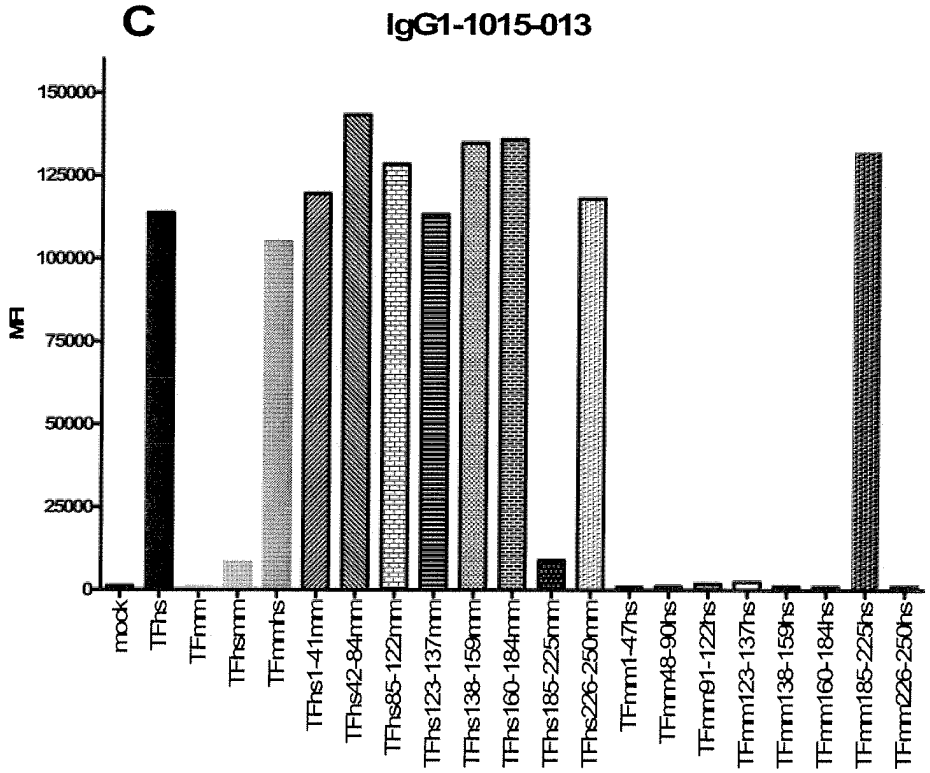


Figure 18 - continued


C
IgG1-1015-013
MFI
150000
125000
100000
75000
50000
25000
0
mock
TFhs
TFmm
TFhsmm
TFmmhs
TFhs1-41mm
TFhs42-84mm
TFhs85-122mm
TFhs123-137mm
TFhs138-159mm
TFhs160-184mm
TFhs185-225mm
TFhs226-250mm
TFmm1-47hs
TFmm48-90hs
TFmm91-122hs
TFmm123-137hs
TFmm138-159hs
TFmm160-184hs
TFmm185-225hs
TFmm226-250hs

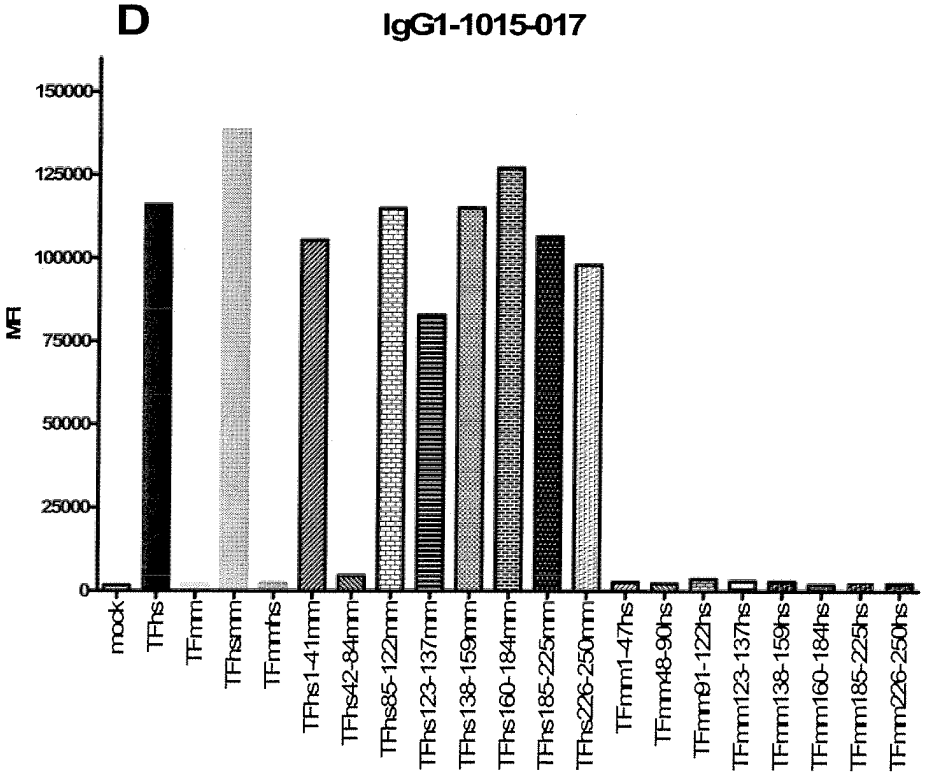

D
IgG1-1015-017
MFI
150000
125000
100000
75000
50000
25000
0
mock
TFhs
TFmm
TFhsmm
TFmmhs
TFhs1-41mm
TFhs42-84mm
TFhs85-122mm
TFhs123-137mm
TFhs138-159mm
TFhs160-184mm
TFhs185-225mm
TFhs226-250mm
TFmm1-47hs
TFmm48-90hs
TFmm91-122hs
TFmm123-137hs
TFmm138-159hs
TFmm160-184hs
TFmm185-225hs
TFmm226-250hs

Figure 18 - continued

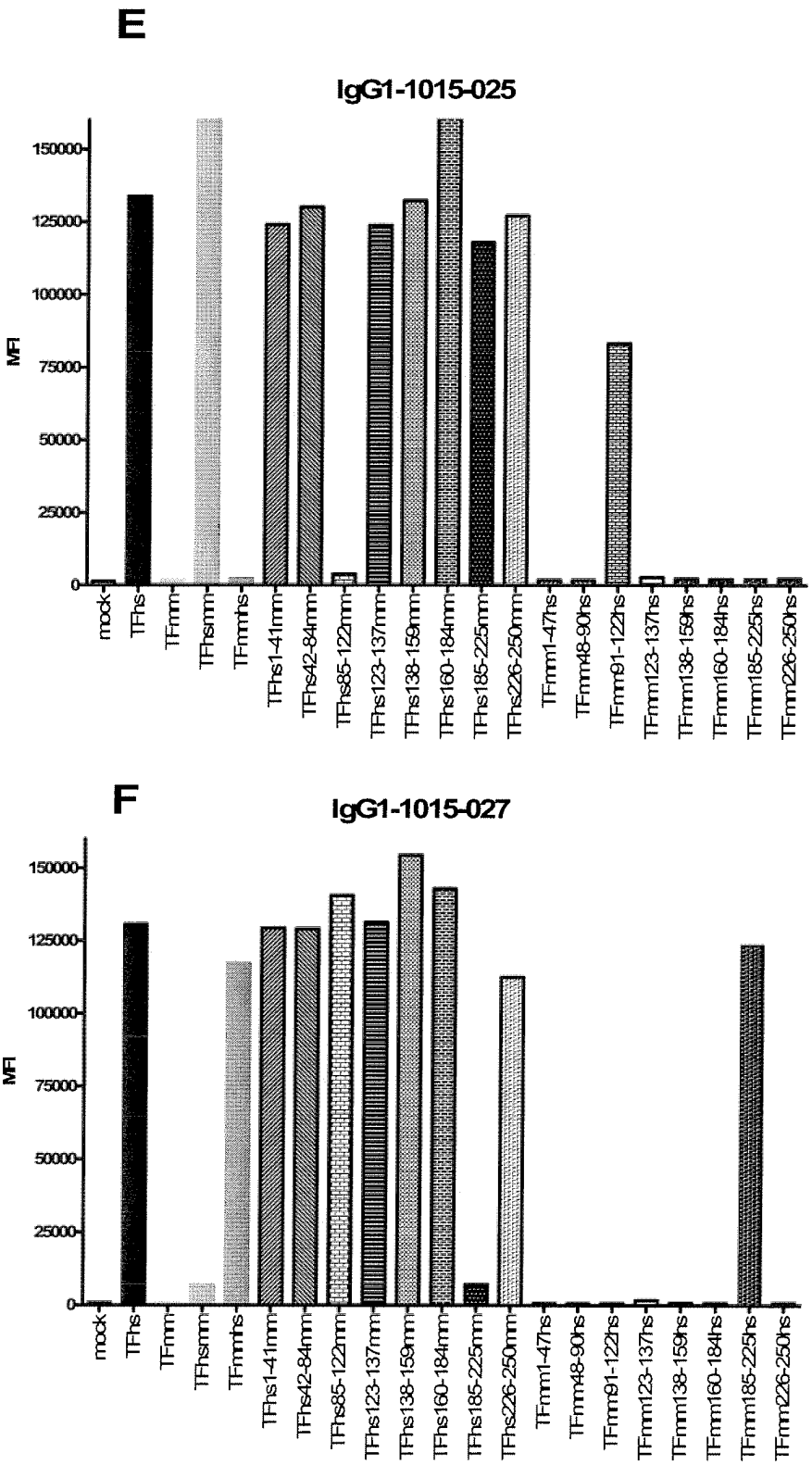


Figure 18 – continued

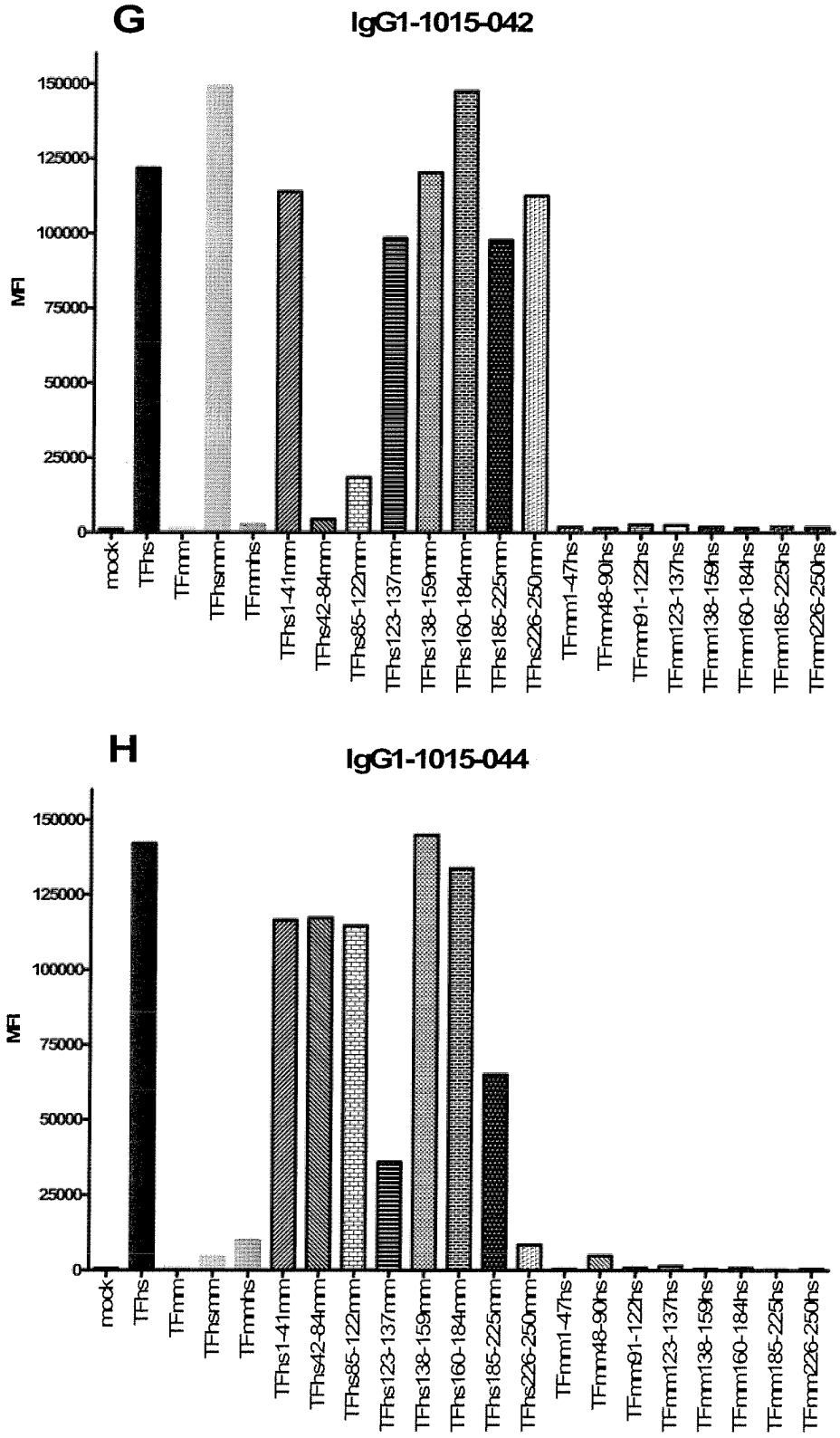


Figure 18 – continued

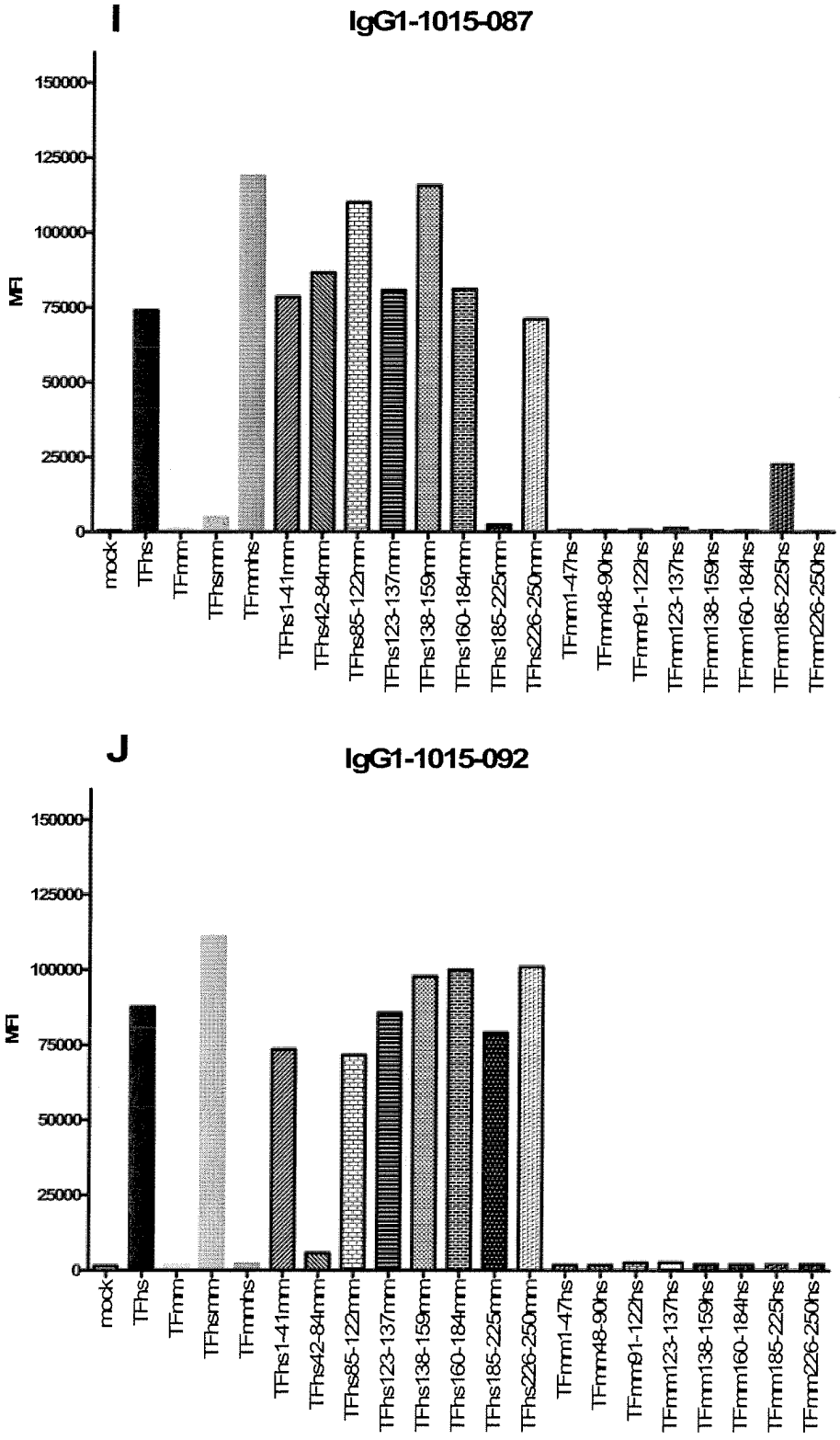


Figure 18 – continued

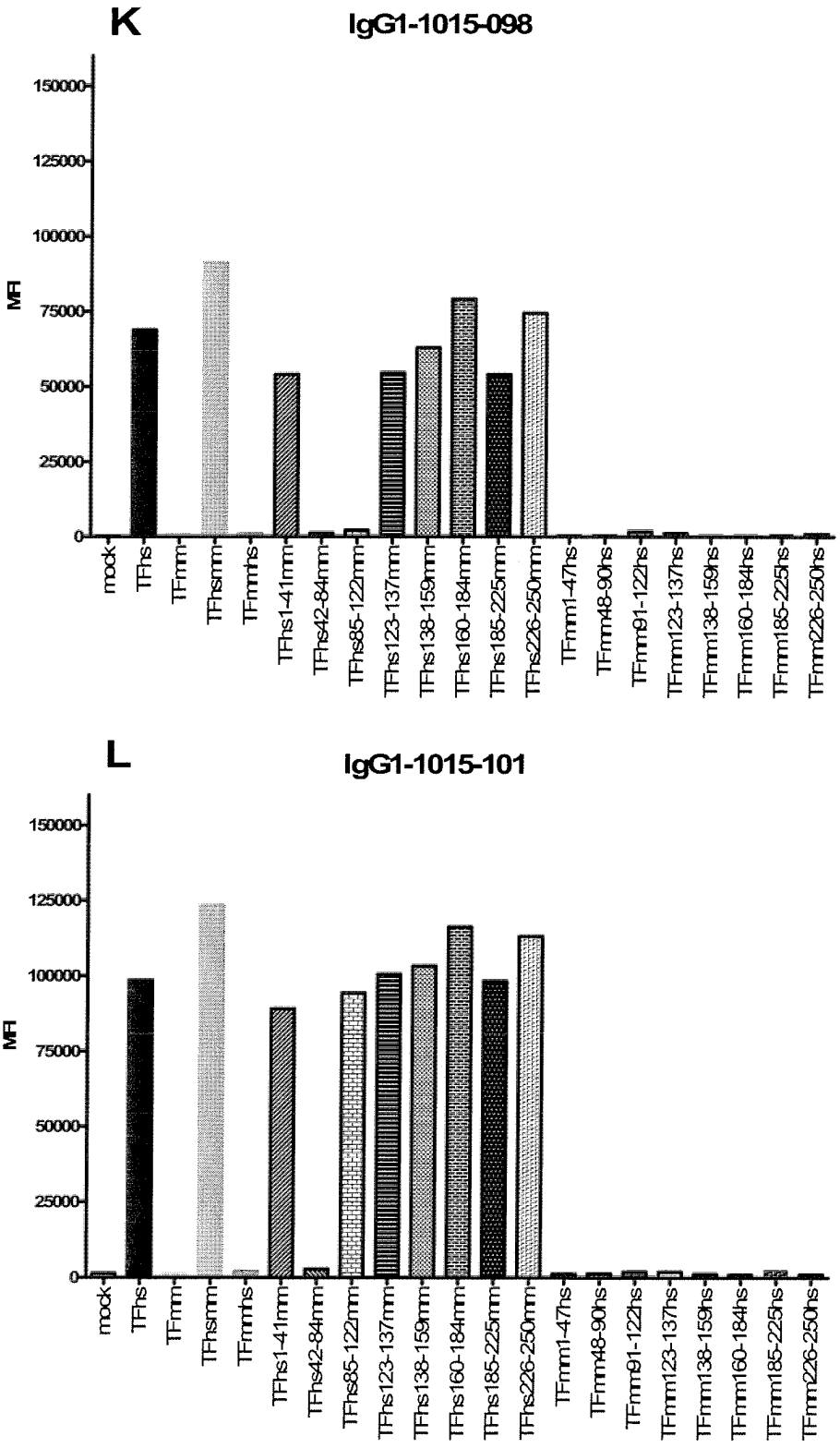


Figure 18 – continued

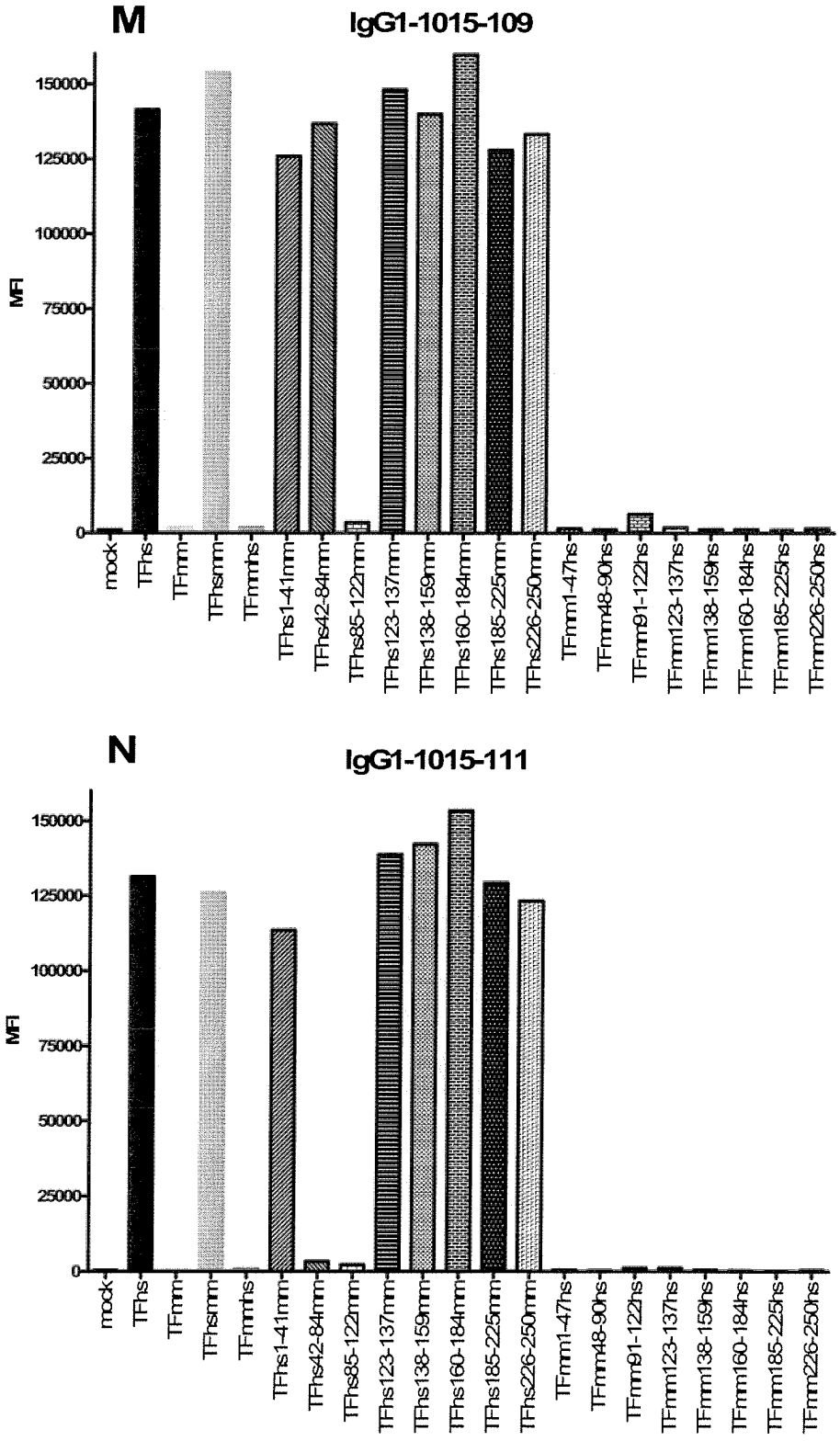


Figure 18 – continued

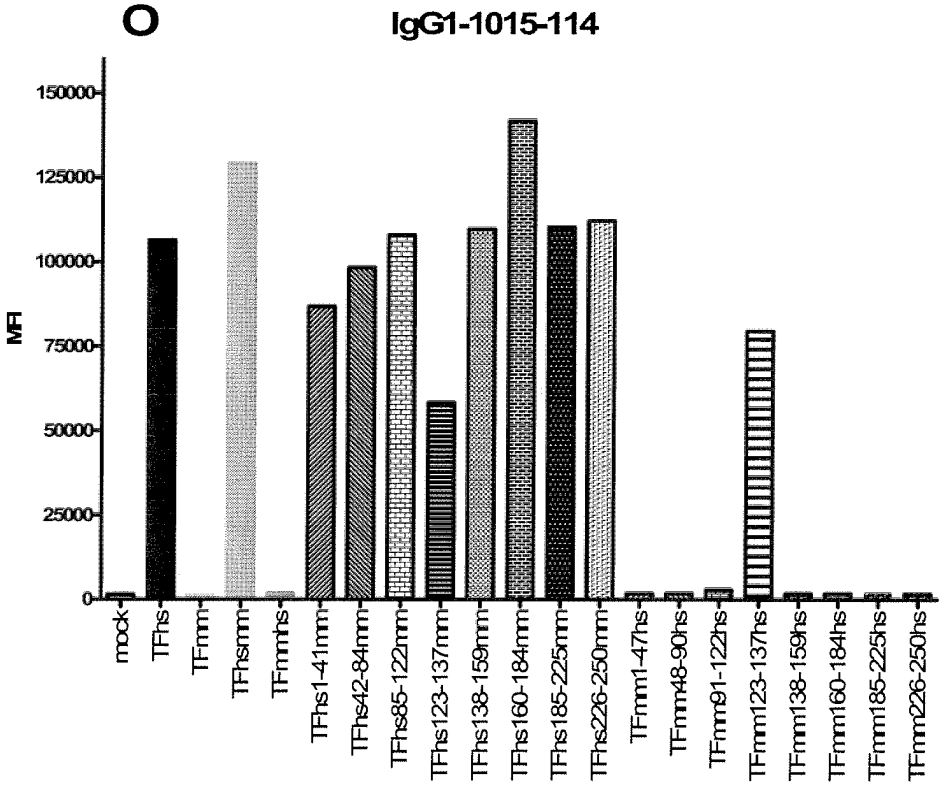


Figure 18 – Binding of anti-TF HuMabs to TF shuffle constructs expressed on HEK293F cells.

Shown are binding profiles of the anti-TF HuMabs to the different TF shuffle constructs expressed on HEK293F cells, as measured by FACS. Each panel shows data from one lead clone. On the x-axis the different constructs are depicted; mock, TFhs, TFmm, TFhsmm, TFmmhs, TFhs1-41mm, TFhs42-84mm, TFhs85-122mm, TFhs123-137mm, TFhs138-159mm, TFhs160-184mm, TFhs185-225mm, TFhs226-250mm, TFmm1-47hs, TFmm48-90hs, TFmm91-122hs, TFmm123-137hs, TFmm138-159hs, TFmm160-184hs, TFmm185-225hs, TFmm226-250hs.

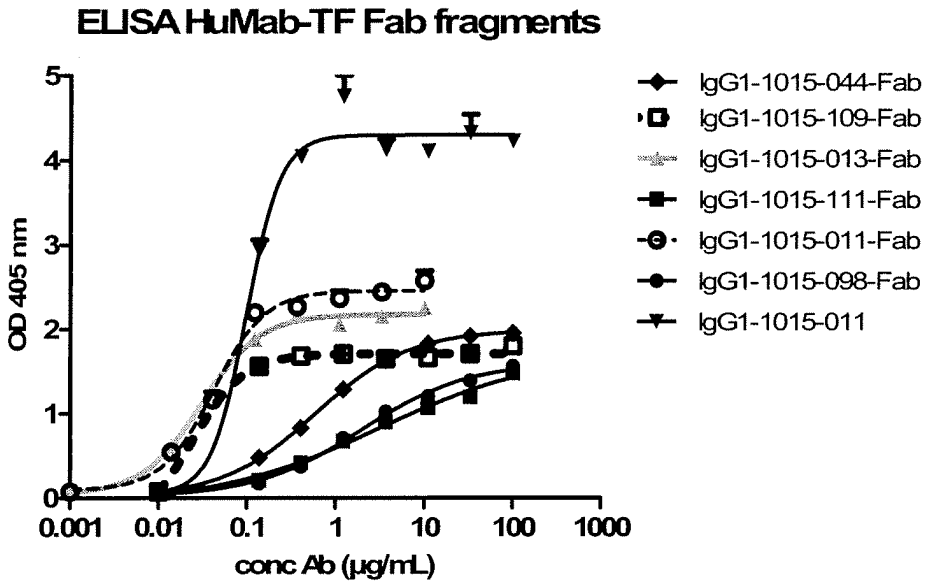


Figure 19. Binding of HuMab-TF Fab fragments to extracellular domain of TF, determined by ELISA.

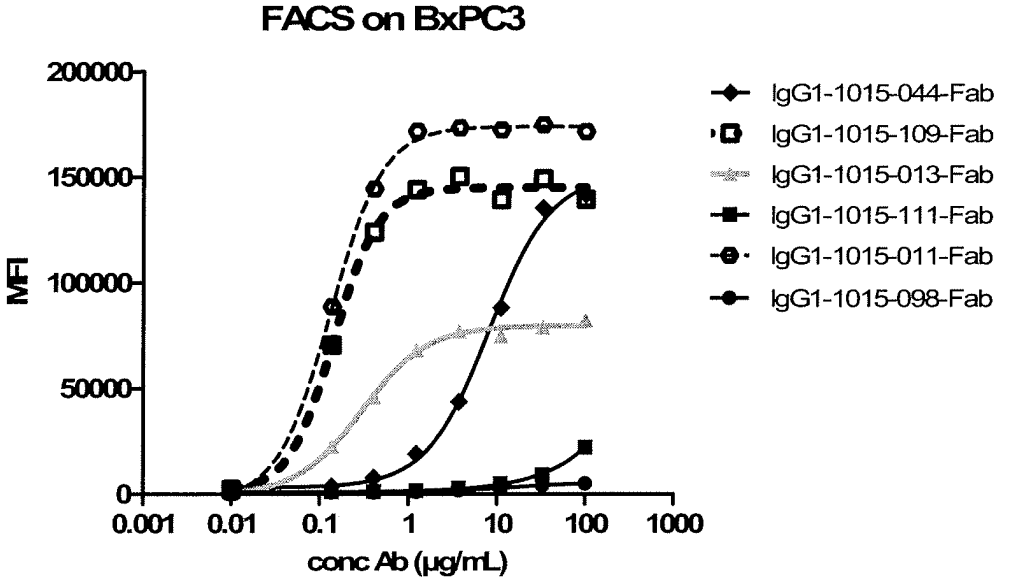


Figure 20. Binding of HuMab-TF Fab fragments to cellular TF, determined by FACS on BxPC3 cells.

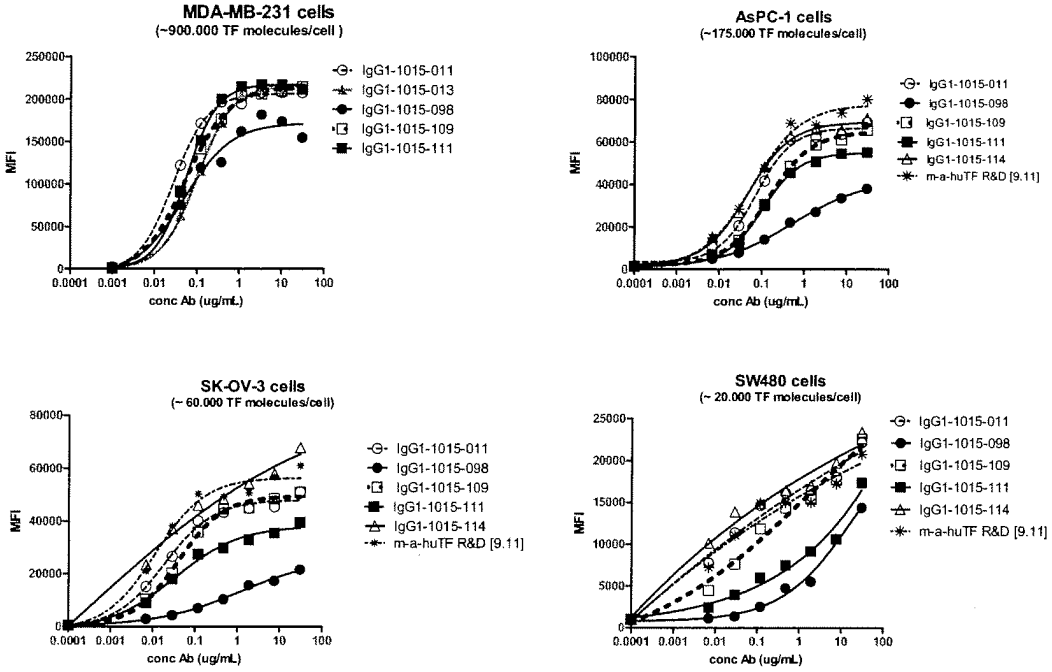


Figure 21. Binding profile of anti-TF HuMabs is dependent on the number of TF molecules expressed.

Binding of anti-TF HuMabs to cell lines expressing different levels of TF was determined by FACS.